



저작자표시-비영리-변경금지 2.0 대한민국

이용자는 아래의 조건을 따르는 경우에 한하여 자유롭게

- 이 저작물을 복제, 배포, 전송, 전시, 공연 및 방송할 수 있습니다.

다음과 같은 조건을 따라야 합니다:



저작자표시. 귀하는 원저작자를 표시하여야 합니다.



비영리. 귀하는 이 저작물을 영리 목적으로 이용할 수 없습니다.



변경금지. 귀하는 이 저작물을 개작, 변형 또는 가공할 수 없습니다.

- 귀하는, 이 저작물의 재이용이나 배포의 경우, 이 저작물에 적용된 이용허락조건을 명확하게 나타내어야 합니다.
- 저작권자로부터 별도의 허가를 받으면 이러한 조건들은 적용되지 않습니다.

저작권법에 따른 이용자의 권리는 위의 내용에 의하여 영향을 받지 않습니다.

이것은 [이용허락규약\(Legal Code\)](#)을 이해하기 쉽게 요약한 것입니다.

[Disclaimer](#)

Master's of Engineering

**GEO-POLYMER CONCRETE SOLIDIFICATION OF FOUNDRY SAND AND  
FLY ASH: CHARACTERIZATION OF HEAVY METAL LEACHING AND  
OPTIMIZATION OF COMPRESSIVE STRENGTH**

The Graduate School of the University of Ulsan  
Department of Civil and Environmental Engineering

**Venkatesan Mayandi**

**GEO-POLYMER CONCRETE SOLIDIFICATION OF FOUNDRY SAND AND  
FLY ASH: CHARACTERIZATION OF HEAVY METAL LEACHING AND  
OPTIMIZATION OF COMPRESSIVE STRENGTH**

Advisor: Professor Hung-Suck Park

A Thesis

Submitted to  
the Graduate School of the University of Ulsan  
*In Partial Fulfillment of the Requirements  
for the Degree of*

Master's of Engineering

By

Venkatesan Mayandi

Department of Civil and Environmental Engineering  
University of Ulsan, South Korea

2017

**GEO-POLYMER CONCRETE SOLIDIFICATION OF FOUNDRY SAND AND  
FLY ASH: CHARACTERIZATION OF HEAVY METAL LEACHING AND  
OPTIMIZATION OF COMPRESSIVE STRENGTH**

This certifies that the thesis  
of Venkatesan Mayandi is approved



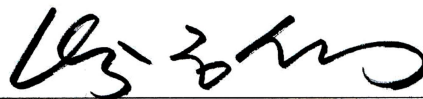
---

Prof. Byeong-Kyu Lee, Committee Chair



---

Prof. Seok Young Oh, Committee Member



---

Prof. Hung Suck Park, Committee Member

Department of Civil and Environmental Engineering  
University of Ulsan, South Korea  
November 2017

## TABLE OF CONTENTS

ABSTRACT .....	7
1. INTRODUCTION .....	9
1.1 Background of study .....	9
1.2 Objective and scope .....	12
1.3 Thesis structure .....	12
2. LITERATURE REVIEW .....	13
2.1 Ordinary Portland cement (OPC).....	13
2.2 Geo-polymer concrete (GPC) .....	14
2.2.1 Geo-polymerization process.....	15
2.2.1 Mechanism of heavy metal immobilization.....	16
2.3 Foundry sand replacement in concrete review.....	17
2.4 Key components of GPC.....	21
2.4.1 Fly ash .....	21
2.4.2 Ground granulated blast furnace slag (GGBFS).....	22
2.4.3 Waste foundry sand.....	23
2.5 Heavy metals in geo-polymer concrete.....	23
2.5.1 Lead (Pb).....	24
2.5.2 Chromium (Cr).....	24
2.5.3 Copper (Cu).....	25
2.5.4 Zinc (Zn) .....	25

2.5.5	Nickel (Ni) .....	26
2.5.6	Iron (Fe) .....	26
2.6	D-Optimization .....	27
3.	MATERIALS AND METHODS .....	29
3.1	Materials.....	29
3.1.1	Cement .....	29
3.1.2	Fly ash .....	29
3.1.3	GGBFS.....	30
3.1.4	Foundry sand.....	30
3.1.5	Fine aggregate .....	30
3.1.6	Coarse aggregate .....	30
3.1.7	Alkaline solution .....	31
3.2	Statistical experimental mixture design .....	31
3.3	Mixture design calculation of GPC.....	33
3.4	OPC and GPC Specimen.....	34
3.4.1	Specimen preparation.....	34
3.4.2	Curing.....	35
3.5	Physico-chemical characterization.....	37
3.5.1	Compressive strength.....	37

3.5.2	Crystal structure and chemical characterization .....	38
3.5.3	Determination of heavy metal content in incineration fly ash .....	39
3.5.4	Heavy metal leaching evaluation .....	40
4.	EXPERIMENTAL RESULTS AND DISCUSSION .....	41
4.1	Heavy metal contents and leaching concentrations .....	41
4.2	Compressive strength .....	49
4.3	FE-SEM &XRD analysis .....	52
4.4	Response surface optimization.....	55
4.5	Statistical results .....	56
4.6	Analysis of responses.....	61
4.7	Implication of the results.....	65
5.	Conclusion .....	67
	REFERENCES .....	69

## LIST OF FIGURES

Figure 1-1 Geo-sand mining in south India.....	10
Figure 2-1 Geo-polymerization process(adapted: Rao & Liu, 2015).....	15
Figure 2-2 Heavy metal immobilization mechanism (adapted: Zhuang et al., 2016) .....	17
Figure 3-1 Cylindrical shaped mold for casting .....	35
Figure 3-2 Curing the specimen .....	36
Figure 3-3 Compressive test machine.....	37
Figure 3-4 Specimen after the compression .....	38
Figure 4-1 Heavy metal leaching for (a) Pb, (b) Cr, (c) Cu, (d) Fe, (e) Ni and (f) Zn .....	48
Figure 4-2 Compressive strength with compression of 7 <sup>th</sup> and 28 <sup>th</sup> day .....	51
Figure 4-3 FE-SEM images .....	53
Figure 4-4 XRD analysis to determine the patterns before solidification .....	54
Figure 4-5 XRD analysis to determine the patterns after solidification .....	54
Figure 4-6 represents the 7 <sup>th</sup> day predicted VS actual compressive strength values .....	59
Figure 4-7 represent 28 <sup>th</sup> day predicted VS actual compressive strength values.....	59
Figure 4-8 7 <sup>th</sup> day normal plot of residuals.....	60
Figure 4-9 28 <sup>th</sup> day normal plot of residuals .....	60
Figure 4-10 7 <sup>th</sup> day contour plot .....	62
Figure 4-11 28 <sup>th</sup> day contour plot .....	62
Figure 4-12 7 <sup>th</sup> day response surface plot.....	63
Figure 4-13 28 <sup>th</sup> day response surface plot.....	63
Figure 4-14 7 <sup>th</sup> day fine aggregate and foundry sand component graph.....	64
Figure 4-15 28 <sup>th</sup> day fine aggregate and foundry sand component graph.....	64



## LIST OF TABLES

Table 2-1 Selected literatures for the application of Response Surface Methodology (RSM) .....	28
Table 3-1 Optimization mixture design (wt%) .....	32
Table 3-2 Mix design of GPC (Unit, Kg in 1m <sup>3</sup> ) .....	34
Table 3-3 Chemical compositions of materials .....	39
Table 4-1 Heavy metals content and leaching concentration of fly ash, foundry sand, and GGBFS .....	42
Table 4-2 KSLP Leaching concentration of heavy metal in different mixing ratios.....	44
Table 4-3 Compressive strength of specimen for various tests and the conventional concrete.....	50
Table 4-4 Statistical analysis of compressive strength in solidified GPC on 7 <sup>th</sup> day .....	57
Table 4-5 Statistical analysis of compressive strength in solidified GPC on 28 <sup>th</sup> day .....	57
Table 4-6 Comparison of heavy metal leaching and compressive strength research finding in cured concrete.....	66

## **ACKNOWLEDGMENT**

I am very Thankful to all the professors in the department of Civil and Environmental engineering. I have learnt a lot from them during course study and valuable discussions.

I am very thankful to my advisor Professor Hung-Suck Park for the financial help, encouragement, support, and valuable suggestions during the entire period of my study and research. His proper and timely guidance, kindness, teaching and motivation made this thesis to be written within due time. Without his guidance, it would not be possible for me to complete this thesis on time.

I am very thankful to all my laboratory members and members of Centre for Clean Technology and Resource Recycling, University of Ulsan for their help, valuable discussions, and providing family like environment during my entire study. I would like to special thanks to our previous lab manager, Mr. JinWoong Beak and lab member Dr. Angelo Earvin Sy Choi, who always helped me whenever I got in trouble or needed help in my research.

I am very thankful to my family members for their prayers, encouragement, help, and motivation during my entire study period. I am very thankful to my elder brother; Nanda Kumar Venkatesan who always encouraged me for my higher studies.

I am very thankful to Dr.Dileep Kumar Appana, who recently completed his doctorate study from University of Ulsan. He was always very helpful during my stay here in Ulsan, South Korea. And I am very thankful to my Korean friend Anhyunji, she was always very helpful during my stay here in Ulsan, South Korea.

## ABSTRACT

This research work evaluated the structural and environmental performance of partial fine aggregate replacement in low calcium fly ash in geo-polymer concrete (GPC), which consequently reduces its carbon footprint. The novelty of this research work is primarily in the utilization of waste foundry sand for partial replacement of fine aggregate in GPC. The brand name for a binder is Geo-Polymer (alkaline solution), which is emerging as an innovative environment-friendly construction material.

In this study, we examined the effect of mixture ratios of ground granulated blast furnace slag (GGBFS), waste foundry sand, and fly ash on GPC characteristics. The cylindrical GPC sample mould size 100×200mm was made based on the statistical experimental design with varying fine aggregate (30–55 wt%), foundry sand (15–40 wt%) and fly ash (20–30 wt%). The total heavy metal concentrations in the material ash are determined by the method defined by Baker and Amacher, while heavy metal leaching by the MBA method and Korean standard leaching method. Field emission-scanning electron microscopy and energy dispersive X-ray diffraction (XRD) were used for the morphological characterization and mineral phase analysis.

The optimum compressive strength of GPC was 19.0Mpa (7<sup>th</sup> day) and 22.2Mpa (28<sup>th</sup> day) from the mixture percentage of 51.9wt% fine aggregate, 24.8wt% foundry sand and 23.3wt% fly ash. Under the same experimental condition, this was higher than that of the conventional concrete which was 16.5Mpa (7<sup>th</sup> day) and 18.5Mpa (28<sup>th</sup> day), respectively. The compressive strength of GPC increased with the increase in curing time

from 7 to 28 days, respectively, which is due to the improved bonding of silicon dioxide and calcium oxide on GPC. Furthermore, cured GPC specimen achieved heavy metal immobilization in the range of 98-100% which is promising for environmental applications. The alkaline solution used for GPC converted the heavy metals compounds in the materials into highly insoluble metal hydroxide and simultaneously encapsulates the fly ash thermal residue. The leaching heavy metal concentration of cured GPC is Pb (0.019mg/l), Cr (0.013mg/l), Cu (0.013mg/l), Fe (0.6mg/l), Ni (0.067mg/l) and Zn (0.02mg/l).

These results ascertained that foundry sand can be used efficiently as an eco-friendly construction material in GPC by substituting raw materials which result in a cost carbon emission reduction. Though, this research shows the potential of substituting fine aggregate by foundry sand, further research are required to practically apply in the real field, considering the field condition and result of this fundamental experimental study.

# 1. INTRODUCTION

## 1.1 Background of study

Fine aggregate (sand) is being depleted at a higher rate to meet the growing demand of large scale infrastructure construction. In Tamil Nadu, a state province in southern India, sand mining is increasing day by day to meet this demand. India's construction works planned to generate \$165 billion of GDP in a financial year and therefore construction materials, especially concrete is required in large amount which consumes millions of tons of sand. New estimates by the researchers and media groups report that it this demand may increase further to 500 million metric tons annually to generate additional \$ 50 billion a year approximately (Rajshekhar, 2017).

With such kind of exploitation of the river sand, the natural river water flow is being destroyed which may lead to devastating neighboring environment and damaging ecosystem. The consequences such as river water not reaching small reservoir and lakes, and therefore effecting farmer's every day agricultural necessities are considerable. During sand mining, heavy metals are leached which degrades the quality of water. Therefore, sand performs an important role in protecting our ecosystem. Our ecosystem is very damaged by sand mining and is required to be protected (Saviour & Stalin, 2012). So this research focus on utilizing waste foundry to replaced fine aggregate. The foundry sand is a high quality silica sand by-product from the production of both ferrous and non-ferrous metal casting industry and creates environmental problems because of its improper

disposal. Thus, its usage in building material, construction and in other fields is essential for reduction of environmental problems. About 12 million tons of waste foundry sand is produced by these casting industries in the United States alone



**Figure 1-1** Geo-sand mining in south India

Moreover, another problem associated with the construction sector is the consumption of cement. After water, the world's most utilized resource or material is Portland cement. The Portland cement is most widely used in the construction sector and during the year 2016 alone, nearly 4200 million metric tons of cement was produced globally. Worldwide, China and India is the world's largest producer of cement. Based on the cement usage and production for the year 2016 worldwide, China produced 2480 million metric tons while India produced 290 million metric tons of cement. So, worldwide 57.2% cement was produced in China, which means China was contributing to half of the production globally. According to Bassi et al. (1999), from cement production industry, 0.87 ton of carbon dioxide is emitted from 1 ton of cement production. As a

result, the construction industry needs alternative binding material to replace the Portland cement for achieving an eco-friendly and ecologically sustainable concrete. Further, studies can be found that have been done to partially or completely replace some material like fly ash, rice husk, GGBFS, etc., in Portland cement. So in this study Portland cement utilized low calcium fly ash (LCFA) and ground granulated blast furnace slag (GGBFS) were used in geo-polymer concrete. However, Geo-polymer cement is a new kind of cement which uses a different chemistry to that found in traditional OPC. A geo-polymer is made by activating amorphous alumino-silicate materials, such as fly ash and slag, with alkali-based chemicals such as sodium hydroxide and sodium silicate. Geo-polymer cement does not need to contain OPC to work. Geo-polymers have been known to be useful binders in concrete for over 60 years. Moreover, CO<sub>2</sub> footprint is approximately 80% lower than OPC cement (Abdel-Gawwad& Abo-El-Enein, 2016). The main advantage use of waste foundry sand and GPC is the reduction in environmental impact to move towards sustainable development which is defined as the optimum usage with the correct and efficient operation of basic and natural resource for providing the requirement of the future generation. Carbon dioxide (CO<sub>2</sub>) emission of geo-polymer concrete is 9% less than OPC

## **1.2 Objective and scope**

The objective of this study includes:

1. To study the performance of partial fine aggregate replacement of waste foundry sand in low calcium fly ash (LCFA) based GPC.
2. To utilize the D-optimal mixing design; different combinations of the mixture i.e. fine aggregate, waste foundry sand and fly ash are generated.
3. The compressive strength of the proposed GPC specimen is measured and compared to the ordinary concrete.
4. Field emission-scanning electron microscopy and X-ray diffraction (XRD) are then carried out to find the heavy metal constituency with the use of fly ash, GGBFS, and foundry sand. Heavy metal leaching analysis is done on this mix to test the immobilization.

## **1.3 Thesis structure**

In Chapter 1, a brief introduction and Chapter 2, the literature review of the GPC has been given and the motivation of the study is discussed. In Chapter 3, material and method has been explained. In Chapter 4, results obtained are explained. In Chapter 5, a conclusion has been made on basis of the experimental result and discussions are given.



## 2. LITERATURE REVIEW

### 2.1 Ordinary Portland cement (OPC)

The generally concrete is the mixed combination of Portland cement, fine aggregate, coarse aggregate, water and mixed together. Portland cement generally referred to as OPC. Worldwide construction and infrastructure area most commonly use OPC cement. OPC is made from grinding to a limestone powder (60-65%) and secondary materials such as sandstone, marl, shale, iron, clay, and fly ash. OPC is made up of four main compounds: tricalcium aluminate ( $3\text{CaO} \cdot \text{Al}_2\text{O}_3$ ), and a tetra-calcium aluminoferrite ( $4\text{CaO} \cdot \text{Al}_2\text{O}_3\text{Fe}_2\text{O}_3$ ), tricalcium silicate ( $3\text{CaO} \cdot \text{SiO}_2$ ), dicalcium silicate ( $2\text{CaO} \cdot \text{SiO}_2$ ). The chemical composition of OPC is lime (CaO) 60-65% and the effect of lime is control strength and soundness, silica ( $\text{SiO}_2$ ) present in 20-25% and use of silica content is increasing the strength, alumina ( $\text{Al}_2\text{O}_3$ ) present in 4-8% make to quick settling an excess amount of  $\text{Al}_2\text{O}_3$  cause lower strength, iron oxide ( $\text{Fe}_2\text{O}_3$ ) 2-4% and its gives colors and helps to blend of compounds, magnesium oxide (MgO) 1-2% and this also gives color and hardness and excess amount of MgO make cracks, sodium oxide ( $\text{Na}_2\text{O}$ ) 0.1-0.5% its controls the residues and sulphur trioxide ( $\text{SO}_3$ ) 1-2% makes cement sounds. This emits high  $\text{CO}_2$  concentration which ranges from 0.66 to 0.82kg of  $\text{CO}_2$  emitted for every kilogram of OPC manufactured.  $\text{CO}_2$  potentially adds the threat towards global warming due to being one of the greenhouse gases. Moreover, the contribution of the production of OPC in general is approximately 5–7% of global anthropogenic  $\text{CO}_2$  emissions

(Mangialardi, Paolini, Poletti, & Sirini, 1999). But in recent years, the theory of concrete is not extended for the development of geo-polymer materials (Davidovits, 1994) has led researchers to ignore green (eco-friendly) concrete, commonly named GPC. GPC generally sources material of fly ash, rice husk, and alkali liquids (used for binders), water, coarse and fine aggregate which are then mixed together.

## **2.2 Geo-polymer concrete (GPC)**

Geo-polymer concrete is a part of a group of concrete and that have been developed since early 1960. Geo-polymer binders may be made from a variety of aluminosilicate sources. The engineering aspects of geo-polymer concrete as described in this document relate to geo-polymeric materials based primarily on low calcium (or Class F) fly ashes, waste foundry sand and GGBFS. While the commercial availability of geo-polymer concrete is a new phenomenon globally, geo-polymer technology and its application in real projects are not new.

The geo-polymer binder is usually formed by the interaction of an alkaline solution i.e. activating solution (or activator) with a reactive aluminosilicate powder. In commercial geo-polymer production, this is usually a mixture of fly ash (waste from coal combustion) and blast furnace slag i.e. wastes from iron-making. The solid powder (binder) partially dissolves into water. The dissolved components rearrange into an aluminosilicate gel which then cross-links and hardens to form the geo-polymer cement. This cement can replace hydrated Portland cement in concrete production. When mixed with coarse and

fine aggregates, a high-performance and lowCO<sub>2</sub> concrete can be produced. This research is carried out to produce a low-cost and eco-friendly GPC.

### 2.2.1 Geo-polymerization process

In the first step of geo-polymerization, aluminate and silicate tetrahedral monomers are generated by alkali dissolution of solid alumino silicate precursors. While in the next stage, the monomers form oligomers which lead to the dissolution of more precursor materials so that the solution is saturated with a complex mixture of silicate, aluminate and alumino-silicate species, which polymerize into an amorphous gel. As shown in Fig 2-1, this gel is then consolidated and hardened into geo-polymers (Rao & Liu, 2015)

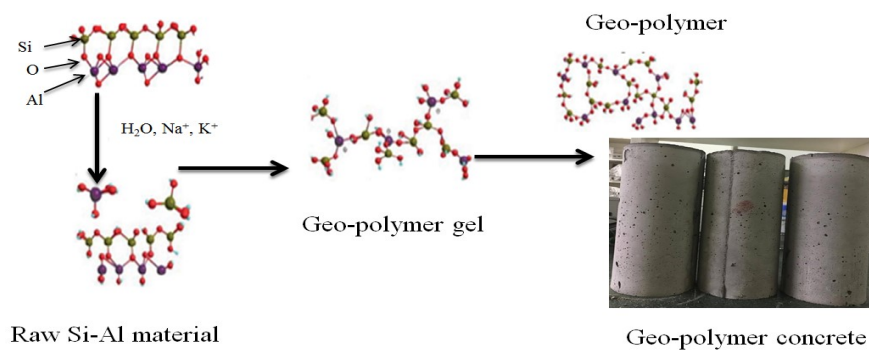


**Figure 2-1** Geo-polymerization process(adapted: Rao & Liu, 2015)

Geo-polymers are new materials for fire- and heat-resistant coatings and adhesives, mechanical applications, high-temperature ceramics, new binders for fire-resistant fiber composites, toxic and radioactive waste encapsulation and new cements for concrete. Geo-polymers are a class of synthetic inorganic alumino silicate materials generally formed by the reaction of an alumino silicate with a silicate solution under strongly alkaline conditions. In these conditions, free SiO<sub>4</sub> and AlO<sub>4</sub> tetrahedral units are generated and

linked to yield polymeric precursors ( $-\text{SiO}_4-\text{AlO}_4-$ , or  $-\text{SiO}_4-\text{AlO}_4-\text{SiO}_4-$ , or  $-\text{SiO}_4-\text{AlO}_4-\text{SiO}_4-\text{SiO}_4-$ ) by sharing all oxygen atoms between two tetrahedral units, while water molecules are released (Roviello et al., 2013). The alkaline solution of sodium hydroxide and sodium silicate act as the geo-polymer gel. This gel increases the capacity of the GPC strength.

### **2.2.1 Mechanism of heavy metal immobilization**

Geo-polymerization is the alternative method to immobilize soluble heavy metals from slag, fly ash, or any other industrial waste. The fly ash GPC hazardous materials (Pb, Cr, Fe, Cu, Zn and etc.,) are tightly attached to the three dimensions structure. The main mechanisms of metal immobilization in fly ash-based geo-polymer are physical encapsulation and chemical stabilization. The physical encapsulation occurs after the heavy metals immobilization treatments, the waste forms resulted towards a low permeable barrier in the contaminations. This then decreases the exposed surface of wastes. The chemical stabilization then happened in the heavy metals which are converted into more stable and less soluble in the metal-bearing phase (Guo, Liu, Yang, & Zhang, 2017). The GPC alkaline solution acted as a geo-polymer gel that immobilizes the heavy metals. The heavy metals were interlocked in alkaline solution so the leaching of metal concentration is reduced in GPC.

Concerned with the environmental issues, the concrete mixture should be checked whether the heavy metals present in fly ash are immobilized through geo-polymerization. Guo et al. (2017) investigated the 3Pb component behaviors alone when dissolved in

sodium hydroxide solution to establish a geo-polymer interface, and confirmed its immobilization. Zhuang et al. (2016) discussed how the mechanism of geo-polymerization (see Fig.2-2) can be improved by fine tuning Si/Al ratios along with alkali solutions, curing conditions and adding slag, fiber, rice hush-bark, ash and red mud.



**Figure 2-2** Heavy metal immobilization mechanism (adapted: Zhuang et al., 2016)

### 2.3 Foundry sand replacement in concrete review

In United States alone, nearly 3000 foundries utilize 100 million tons of sand in its production leaving waste foundry sand as residue (Siddique, Schutter, & Noumowe, 2009; Torres-Carrasco & Puertas, 2015; Bhardwaj & Kumar, 2017). Such over exploitation has risen to alarming levels especially at vulnerable locations. Due to which several governments have imposed a restriction on sand mining and have raised its price. These limitations directly impact the construction industries with increased production costs. Therefore, potential replacements are being investigated with partial or complete replacement of concrete material fine aggregate (Dolage, et.at., 2013). As such, ten selected literatures are reviewed as follows:

- 1) Gurumoorthy & Arunachalam (2016) investigated the mechanical and micro structural properties of waste foundry sand as a replacement of fine aggregate to improve the strength of ordinary concrete.
- 2) Siddique & Noumowe (2008) and Siddique & Singh (2011) utilized this industrial by product waste as controlled low-strength materials for managing the scarcity of land-filling. By conducting durability tests they found waste foundry sand and fine aggregate to have similarity in strength and conducted it as an effective replacement. Concrete is widely used in built environment. Efforts are made to preserve the performance of the embodied energy of concrete with the consideration of environmental and cost aspects (Calle, Alho, & Benito, 2017).
- 3) Mangialardi, & Sirini, (1999)utilized waste foundry sand as a partial replacement of fine aggregate in geo-polymer concrete. The percentage of replacement are 0%, 5%, 10%, 15%, 20% and 25% by weight of fine aggregate by waste foundry sand. In this study, 7 day and 28 day compressive strength, split tensile strength and flexural tensile strength of samples was found out.
- 4) Moonet al. (2005) investigated two types of waste foundry sands like clay-bonded sand (CLW) and silicate bonded sand (COW) as a fine aggregate for concrete basic properties such as air contents, setting time, bleeding, workability and slump loss of the fresh concrete, waste foundry sand were tested and compared with those of the concrete mixed without waste foundry sand. Also, compressive strength and tensile strength of hardened concrete was measured. The compressive strength decreased with increasing the replacement of silicate bonded sand and clay-bonded sand. They

further demonstrate the use of waste foundry sand as a partial replacement by fine aggregate in concrete. An experimental investigation was carried out on a concrete containing waste foundry sand in the range of 0%, 20%, 40%, and 60% by weight for M-25 grade concrete. The material was produced, tested and compared with conventional concrete in terms of workability and strength. These tests were carried out on standard cube of 150x150x150mm for 7, 14 and 28 days to determine the mechanical properties of concrete. Through experimental result, they conclude that the compressive strength increases with increase in partial replacement of waste foundry sand and split tensile strength decreases with increases in the percentage of waste foundry sand. Studies showed positive impact of mixing concrete with waste foundry sand, GPC.

- 5) Bakharev, (2006) the following are some of the basic properties of fly ash based GPC. A compression value of GPC depends upon time and type of curing i.e. the age of curing and temperature to which moulds are subjected. There is an increment in compressive strength with increment in a time of curing and temperature. Geopolymer moulds have better greater durability and thermal strength characteristics.
- 6) Siddique et al.(2009) utilized waste foundry sand as partial replacement in ratios of 10%, 20 % and 30% in self-compacting concrete, where the final concrete specimen is subjected to compressive strength, splitting-tensile strength, flexural strength, and modulus of elasticity were determined at 28, 56, 91, and 365 days. Test results indicated a marginal increase in the strength properties of plain concrete by the inclusion of waste foundry sand as partial replacement of fine aggregate.

- 7) Aggarwal & Siddique (2014) waste foundry sand with fine aggregate and bottom ash partially with cement in conventional concrete. The replacement ratios for waste foundry sand were 10 to 50%, and bottom ash was 5 to 30 %. Moreover, the concrete strength was observed that the greatest increase in compressive, splitting tensile strength, and flexural strength compared to that of the conventional concrete was achieved by substituting 30% of the natural fine aggregates with waste foundry sand.
- 8) Madhavan & Vijayprakash (2016) OPC is replaced by 20, 40 & 60% replacement of Fly ash and 30% of fine aggregate is replaced by the waste foundry sand in M25 grade concrete with Conplast 430 admixture. During Phase-I, the compressive strength and split tensile strength of concrete mix at 7<sup>th</sup>, 14<sup>th</sup> and 28<sup>th</sup> day of curing period is determined along with the workability property of fresh concrete and results are analyzed and compared with the conventional concrete and the result was 30% waste foundry sand and 40% fly ash is found to be the optimum percentage at which the cement and fine aggregate can be replaced.
- 9) Associate & Budhgaon (2017) replaced waste foundry sand by varying it from 0-50% in steps of 5% by fine aggregate in ordinary concrete. The compressive strength test was carried on 7<sup>th</sup> and 28<sup>th</sup> day and the compressive strength was increased after replacing the fine aggregates with the certain percentage of foundry sand.
- 10) Torreset al. (2017) utilized waste foundry sand ratios of 10%, 20% and 30% partial replacement of fine aggregate in plain cement concrete. Similarly, splitting tensile strength, flexural strength, compressive strength, and modulus of elasticity tests



were executed on 7<sup>th</sup>, 14<sup>th</sup> and 28<sup>th</sup> day to ensure the specimens strength. The result has shown the no impact on the mechanical performance of plain cement concrete up to 30% for individual replacement or 20% combined.

## **2.4 Key components of GPC**

### **2.4.1 Fly ash**

Fly ash (FA) is a by-product from thermal power generation plants. These plants use different type of coal such as lignite, sub-bituminous, bituminous, and anthracite. Coal used in these power plants is mainly comprised of carbon, oxygen and hydrogen, nitrogen and sulfur (small components) and 10~40% of non-combustible impurities that are present such as clay, quartz, feldspar, shale, and lime. The combustible element of the coal is burnt off by coal as it passes through the high-temperature zone of coal hotspots, while mineral impurities of coal molecules produce various crystalline phases of melted ash. The molten ash cools rapidly when the molten ash is entrained into flue gases leaving the combustion zone from 1500°C~2000°C and in several seconds it is rounded to glassy particles. Utmost of certain particles fly away among the flue gas stream and are therefore called fly ash (Madhavan & Vijayprakash, 2016; Calle et al., 2017).

According to the coal type used, two types of the fly ash are produced. Residue from Anthracite and bituminous coal are classified as class F. Bituminous coal is a thick sedimentary rock, normally looks black, but sometimes its looks dark brown, frequently

with great-defined bands of bright and dull material. Its density is medium hard, moisture content is less and carbon content within 34 ~ 86%.

Less than 6% of the content of calcium oxide (Cao) class F fly ash is referred to as low calcium ash and does not have self-hardening capability and generally reveals pozzolanic properties. It is used to produce air entrained concrete to improve freezing-thawing durability. It usually requires water and reduced hydration heat. Class F fly ash concrete also reveals resistance to Sulfate attack(Khan, et al., 2016). Burning of lignite or bituminous coal generates class C fly ash. Class C fly ash, usually containing 15% Cao, also is called high calcium ash. Class C Fly ash is not just pozzolanic in nature, but self-cementitious (Jiang & Malhotra, 2000; Bakharev, 2006).

#### **2.4.2 Ground granulated blast furnace slag (GGBFS)**

Ground granulated blast furnace slag is sometimes referred to as (GGBFS). The GGBFS is byproduct from steel casting industry. It is obtained by quenching molten iron slag from a blast furnace in water or steam, dried and ground into a fine powder. Blast furnace slag is composed of silicates and alumino silicates of lime (Pavani, et al., 2016). It is a latent hydraulic product which can be activated with lime or Portland cement. GGBFS can increase the abilities to prevent water penetration and chloride penetration, and it can improve the durability of concrete structures. It is an excellent binder to produce high performance cement and concrete.

### **2.4.3 Waste foundry sand**

Waste foundry sand is a major by-product of the metal casting industry and has been successfully utilized as a land filling material for many years. But the use of waste foundry sand for land filling is becoming a problem due to the rapid increase in its disposal cost. Waste foundry sand primarily consists of high-quality uniformly sized silicon sand, which is bonded to the molds for ferrous (steel and iron) and non-ferrous (brass, aluminum, copper) metal casting. Molding and casting operations utilize high-quality silica foundry sand. The molding sands are reused and recycled many times during the casting method. However, the recycled sand deteriorates to the limit that it can no longer be reused in the casting method and it is removed from the foundry and called as waste foundry sand. The automotive manufacturing and its component suppliers are the main generators of foundry sand (Siddique et al., 2009; Associate & Budhgaon, 2017; Bhardwaj & Kumar, 2017).

### **2.5 Heavy metals in geo-polymer concrete**

The rapid increase in toxic heavy metal ions such chromium (Cr), iron (Fe), copper (Cu), lead (Pb), nickel (Ni), and zinc (Zn) their release into the environment and impact on human health is well known. Therefore, these are considered major environmental problems throughout the world as exposure to high levels of toxic heavy metal ions can cause schizophrenia, neurological disorders, cancer, kidney failure, skin disorders, and lung disease, while damaging the function of arteries, DNA, and liver. Considering this danger, many strategies have been established to control levels of toxic heavy metal ions

in various systems via establishing scientific toxicity standards and exposure guidelines such as those from the World Health Organization (WHO) and Environmental Protection Agency (EPA) of United States. In this study the fly ash used contains large amounts of heavy metals such as Pb, Cr, Cu, Fe, Ni, and Zn. The characteristics of each heavy metal are as follows.

### **2.5.1 Lead (Pb)**

Lead is a bluish-white bright metal. It is soft, very thin, flexible, and a comparatively poor conductor of electricity. It is highly resistant to corrosion but tarnishes on-air exposure. The final isotopes are the final products of each of the three sequence of naturally occurring radioactive organs.

Lead is the leading component of lead-acid batteries used in car batteries. It is the traditional base metal for element process pipes, and it is used in electrolysis operation. The computer and television screens have its mainstream application. Other uses are in cables, patches, and lead crystal glassware, ammunition, bearings and sports equipment.

### **2.5.2 Chromium (Cr)**

Chromium is an annoying, fragile and dense metal. Its colour is silver grey and very shiny. When it is heated it pollutes the air which creates green chromium oxides. Chromium is weak in oxygen, which quickly generates a permeable oxide layer. Many environmental and health problems have been associated with Cr in the past as well.

### **2.5.3 Copper (Cu)**

Copper is a red metal with a cubic crystal structure in the face. It was found in periodic table I B group, and silver and gold are accompanied. Copper has low chemical efficiency. In the wet air, a green cover film is formed. This cover shields the metal from additional attack. Most copper compounds will settle and be bound to either water sediment or soil particles. Soluble copper compounds form the largest threat to human health. Usually water-soluble copper compounds occur in the environment after release through application in agriculture.

### **2.5.4 Zinc (Zn)**

Zinc is a glossy blue-white metal. It is found in the periodic table in II B group. It is fragile and crystalline at normal temperatures, but when it is hot between 110°C and 150°C it is perforated and thin. It is a highly reactive metal that acts with dilute acids to produce the hydrogen that connects with oxygen and other non-metals.

It is mainly used for iron storage, 50% of metal zinc goes into steel galvanic, but it is important in producing some alloys. It is used for the negative plates in any electric batteries and to roofing and gutters in building construction. Zinc is a trace element that is essential for human health. When people absorb too little zinc they can experience a loss of appetite, decreased sense of taste and smell, slow wound healing and skin sores. Zinc-shortages can even cause birth defects.

### **2.5.5 Nickel (Ni)**

Nickel is a silver-white, hard, thin and flexible metal. It is one among the iron group and it gets tremendous shine. With heat and electricity it is a very good conductor. Nickel's main application is in the production of alloys. Nickel alloys are classified by toughness, flexibility, and resistance to heat and corrosion. Approximately 65% of the western world is used nickel to produce the alloy and its mixture may vary but 12% of nickel goes to super alloys. The remaining 23% consumption includes alloy steels, rechargeable batteries, catalysts and other chemicals, coin, foundry products and plating.

### **2.5.6 Iron (Fe)**

Iron is a lustrous, ductile, malleable, silver-gray metal (group VIII of the periodic table). Pure iron is a silver-white, textured and malleable metal, which can be made of thinner tubes than cigarette paper. Iron is divided into pure iron, steel and cast iron. Iron is very rare in the natural world and it is difficult to make it by smelting. Iron has been reported to be involved in the inhabitation of fatigue and infection as well as in the development of growth and cognitive ability by being required for the various physiological regulation ability of the human body. Iron can be found in meat, whole meal products, potatoes and vegetables. The human body absorbs iron in animal products faster than iron in plant products. Iron is an essential part of hemoglobin; the red coloring agent of the blood that transports oxygen through our bodies.

## **2.6 D-Optimization**

D-optimal mixture design utilize the response surface methodology (RSM) and can provide multivariate mixture design of construction materials for statistical analysis of concrete mixture optimization (Eriksson, Johansson, & Wikström, 1998; Muteki, MacGregor, & Ueda, 2007). The statistical program of Design-Expert with version 6.0.8 is utilized to derive optimized conditions according to the blending design cost. 14 design blend ratios were designed. Among the 14 compounding ratios set out, 10 items were analyzed according to the above mentioned compressive strength test method, except for overlapping items, and the optimum compounding ratio and predicted compressive strength were investigated. Optimization of the blending ratio was achieved by selecting the mixing ratio of each material through the Cubic model (Choi et al., 2014; Son, Baek, Choi, & Park, 2017; Subramonia Pillai, Kannan, Vettivel, & Suresh, 2016)

**Table 2-1** Selected literatures for the application of Response Surface Methodology (RSM)

<b>Study Focus</b>	<b>Design</b>	<b>Parameters</b>	<b>Main effect</b>	<b><math>R^2</math></b>	<b>Ref.</b>
Optimization of solidification/stabilization treatment of ferro-alloy waste products through factorial design	Central Composite Rotational Design	a. Water/solids b. Cement content c. Curing time (days)	strength and leach resistance	0.94	(Cohen, Cilliers, & Petrie, 1997)
Waste stabilization/solidification of an electric arc furnace dust using fly ash-based geo-polymer	Central composite design	a. Untreated fly ash b. Washed fly ash	Setting time, mechanical strength, and leaching properties.	-	(Mangialardi et al., 1999)
Thiomer solidification of an ASR bottom ash: Optimization based on compressive strength and the characterization of heavy metal leaching	D-optimal hybrid design	a. Thiomer, b. ASR bottom ash c. sand	Compressive strength	0.96	(Son et al., 2017)
Solidification/stabilization of ASR fly ash using Thiomer material: Optimization of compressive strength and heavy metals leaching	D-optimal hybrid design	a. Thiomer, b. ASR fly ash c. sand	Compressive strength and heavy metals leaching	0.9975	(Baek, Choi, & Park, 2017)



### **3. MATERIALS AND METHODS**

This chapter describes the materials used in concrete, statistical experimental mixture design, OPC and GPC specimen, and physico-chemical analyses.

#### **3.1 Materials**

The following materials are used in OPC and GPC specimen.

##### **3.1.1 Cement**

There are different standards of Portland cement available for various purposes. There are also different classes of cement being in OPC. OPC can be categorized such as 33grade, 43 grades, or 53 grades. 53 grades OPC can be collected from any construction material shop which is used for the experimentation. The specific gravity of cement is 3.08.

##### **3.1.2 Fly ash**

Fly ash is a by-product from thermal power plants. Based on the composition of coal, two types of fly ash are produced i.e. class C and class F. Low calcium fly ash is collected from incineration plant at Ulsan, Korea. Fly ash which used to replace cement and the following tests were carried out on fly ash. The specific gravity of fly ash is 2.23.

### **3.1.3 GGBFS**

The blast furnace slag which is a by-product of the iron manufacturing (i.e., GGBFS) is collected from Ulsan Steel Mill Company, Ulsan, South Korea. GGBFS which is also used to replace the cement and the specific gravity of GGBFS is 2.97.

### **3.1.4 Foundry sand**

Waste foundry sand is a high-quality Silica sand of uniform size having bonds of ferrous and non-ferrous metal castings. Foundry was collected from Busan Susek Company, Ulsan, South Korea respectively. Waste foundry sand was used to replace as fine aggregate and the specific gravity of foundry sand is 2.71.

### **3.1.5 Fine aggregate**

In the present investigation, the river sand available near Ulsan was used as fine aggregate. And the sample two tests were carried out sieve analysis and specific gravity test. The fineness modulus and specific gravity of fine aggregate is 2.71.

### **3.1.6 Coarse aggregate**

In the present investigation, locally available crushed blue granite stone aggregate of size 12.5mm was used and the sample two tests were carried out sieve analysis and specific gravity test. The fineness modulus of course aggregate is 6.56 and specific gravity of coarse aggregate is 2.75.

### **3.1.7 Alkaline solution**

In the present study we have used a combination of sodium hydroxide (NaOH) and sodium silicate ( $\text{Na}_2\text{SiO}_3$ ) solutions. The sodium hydroxide solids were technical grade in flakes form (3 mm) with 98% purity was collected from OCL Company Ltd., (Korea). The sodium hydroxide solution was prepared by dissolving either the flakes or the pellets in the portable water. The sodium hydroxide solution was dissolved into portable water. The mass of sodium hydroxide solution is modified depending on the concentration of the solution conveyed in terms of molarity (M). Molar concentrations or molarities are commonly defined as solute in per liter of solution. To use in wide applications, it is defined by an amount of solute per unit volume of solution (Madhavan, 2016; Pavani et al., 2016).

## **3.2 Statistical experimental mixture design**

The D-optimal design process for mixture designs works exactly the same way as that described for RSM design. The design points are selected to minimize the variance associated with the estimates of the coefficient in the specified model. The design space is defined by the low and high-level constraints on each factor and any multifactor constraints. The design of GPC mix is tabulated in Table 3.1. In order to reduce the usage of the fine aggregate, the proposed method included the usage of them as a partial replacement. To maintain the compressive strength of the final concrete mix, the

percentage of fly ash, fine aggregate, for the 830.4 kg/m<sup>3</sup> to be used is tested at different mixture combinations (Bakharev, 2006).

**Table 3-1** Optimization mixture design (wt%)

<b>Run</b>	<b>Fine aggregate</b>	<b>Foundry sand</b>	<b>Fly ash</b>
R1	55.0	15.0	30.0
R2	55.0	15.0	30.0
R3	37.8	33.6	28.6
R4	47.7	30.5	21.8
R5	30.3	39.7	30.0
R6	42.5	27.5	30.0
R7	55.0	23.3	21.7
R8	34.8	40.0	25.2
R9	41.5	38.5	20.0
R10	42.5	33.3	24.2
R11	48.9	24.4	26.7
R12	30.3	39.7	30.0
R13	55.0	23.3	21.7
R14	41.5	38.5	20.0
PP*	51.9	24.8	23.3

***\*PP – Point Prediction***

The design expert 7.0.0 used to optimize the design mixtures compound, fine aggregate (A: 30-55 wt%), WFS (B: 15-40 wt%) and fly ash (C: 20-30% wt%) over the compression strength (Y: KN) in GPC casting. The design mixture has an entirety of 14 test runs which comprise ‘lack of fit estimation’ (4 runs), ‘replicates’ (4 runs), and ‘minimum model points’ (6 runs). The quadratic model obtained from the regression analysis shown in equation 1, defines the relationship between the minor and major variables.

$$Y = \sum \beta_i X_i + \sum \beta_{ij} X_i X_{ij} \dots\dots\dots \text{Eq (1)}$$

Where,  $\beta_i$  and  $\beta_{ij}$  are the interacting factors and the coefficient extended. The statistical result is investigated using the analysis variance (ANOVA). Using the D-optimal design software, this can determine the optimal combination of the three materials in the mixture. This is tabulated in Table 3-1. The standard procedure for solidification can be referred to past literature (Bakharev, 2006; Torres-Carrasco & Puertas, 2015; Vijai et al., 2010).

### 3.3 Mixture design calculation of GPC

In this design, GPC comprises of 75 to 77% of the combined aggregate. The combined aggregate is a combination of foundry sand, fine aggregate and coarse aggregate. The OPC concrete also have the combined aggregate with similar percentage. Normally OPC and GPC have 30% fine aggregate and 45% coarse aggregate, but for this research study foundry sand is being replaced partially with 15 -40 % of the total weight of fine aggregate. The OPC and GPC unit weight of concrete density was found to be 2400kg/m<sup>3</sup>. The ratio of alkaline liquid to fly ash was found to 0.4. The ratio of sodium silicate solution to sodium hydroxide solution was fixed as 2.5 to obtain the mass of sodium hydroxide and sodium silicate solution (Jiang & Malhotra, 2000). An alkaline solution is prepared by sodium hydroxide solution of 8 molarity (8M) with weight of 320 gram (8×40 i.e. molarity × molecular weight) of sodium hydroxide was dissolved into one liter of water. For GPC casting, one day prior preparation of sodium hydroxide solution is

required. Later, the prepared sodium hydroxide solution was mixed with sodium silicate solution. The trial mixture (fly ash 16.4%, fine aggregate 23.0%, coarse aggregate 54.0%, NaOH 1.9%, and Na<sub>2</sub>SiO<sub>3</sub> 4.7% is designed as below and overall values are tabulated in Table 3-2.

**Table 3-2** Mix design of GPC (Unit, Kg in 1m<sup>3</sup>)

<b>Alkaline liquid ratio</b>	0.45
<b>Fly ash</b>	394.3
<b>Fine aggregate</b>	552
<b>Coarse aggregate</b>	1296
<b>NaOH</b>	45.06
<b>Na<sub>2</sub>SiO<sub>3</sub></b>	112.7
<b>Water to solid ratio</b>	0.21

### **3.4 OPC and GPC Specimen**

#### **3.4.1 Specimen preparation**

The GPC solids compounds of fly ash, foundry sand, fine aggregate, GGBFS and coarse aggregate were mixed in a pan mix for 2 to 3 minutes. After dry mix, the alkaline solution is added; water is added continuously until the dry mix changes to wet mix. Such wet mix is blended for around 4 minutes The OPC dry mix has been mixed about 2minutes. Later water is added and continuously mixed another 5minutes for the dry mix to change to wet mix by following the method employed by past studies The mixture was pour into the cylindrical GPC plastic mould size 100×200mm, and table vibrator also used for

settling the concrete via (compaction) (Vijai, Kumutha & Vishnuram, 2010; Madhavan & Vijayprakash, 2016; Torres et al, 2017; Guo et al., 2017).

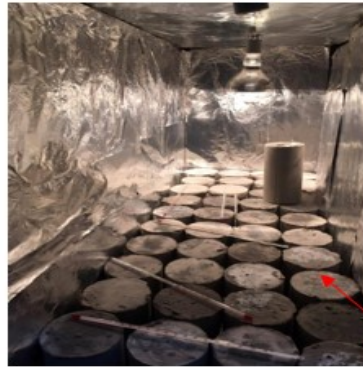
### 3.4.2 Curing

Hot curing and water bath curing were used in the GPC and OPC. After casting GPC specimen were kept in ambient hot temperature room at 24 hours. The ambient room temperature was maintained 60°C to 70°C. After 24 hours the GPC specimen was taken from ambient room temperature and the specimen was remolded. Later it is kept at room temperature (23°C to 30°C) until further testing the specimen is done. The specimen was tested on 7<sup>th</sup> and 28<sup>th</sup> day. After 24 hours the OPC specimen which is remolded is put into water bath curing until testing the specimen as done previously (Khan et al., 2016). In figure 3-1 the cylindrical moulds used for casting can be seen. Figure 3-2 the procedure used for curing ((a) hot temperature (b) room temperature) is shown.



**Figure 3-1** Cylindrical shaped mold for casting

Specimen in Hot Chamber



Cylindrical Concrete Specimen

Specimen at room temperature



**Figure 3-2** Curing the specimen



## 3.5 Physico-chemical characterization

### 3.5.1 Compressive strength

Two types of cylinder specimen are utilized, one is using controlled concrete and the other one is using GPC. The cylinder specimens of size 100mmx200mm are tested by compression testing machine after 7 and 28 days of curing. Samples were weighed before being put in the compression testing machine. The Load was then applied until failure and the crushing load (KN) was noted. The compressive test machine is shown in figure 3-3. The specimen after the compressive strength test is shown in figure 3-4.



**Figure 3-3** Compressive test machine



**Figure 3-4** Specimen after the compression

### **3.5.2 Crystal structure and chemical characterization**

In this study, crystal structure and chemical properties of each sample were analyzed according to mixing design ratio. The crystal structures were compared and analyzed by FE-SEM / EDS in order to understand the binding state, elemental analysis and distribution of each sample by GGBFS concrete. The magnifications of SEM and EDS were set to 100 times and 500 times, respectively. After solidification, samples were placed in a mortar and thoroughly pulverized, and then the particles of the powder were analyzed using an X-ray diffractometer. Table 3-3 shows chemical compositions of various materials in fly ash, foundry sand and GGBFS.

**Table 3-3** Chemical compositions of materials

<b>Chemical composition</b>	<b>Fly ash (wt. %) (Khan et al., 2016)</b>	<b>Foundry Sand (wt. %) (Siddique et al., 2009)</b>	<b>GGBFS (wt. %) (Khan et al., 2016)</b>
SiO <sub>2</sub>	66.56	87.91	31.52
Al <sub>2</sub> O <sub>3</sub>	22.47	4.7	12.22
Fe <sub>2</sub> O <sub>3</sub>	3.54	0.94	1.14
CaO	1.64	0.14	44.53
MgO	0.65	0.3	4.62
Na <sub>2</sub> O	0.58	0.19	0.21
K <sub>2</sub> O	1.75	0.25	0.33
TiO <sub>2</sub>	0.88	0.15	1.03
SO <sub>3</sub>	0.1	0.09	3.24
Loss on ignition (LOI)	1.66	0.02	0.79

### 3.5.3 Determination of heavy metal content in incineration fly ash

The total heavy metal concentrations in the fly ash are determined by utilizing the method defined by Baker and Amacher (Baker & Amacher, 1982; Hseu et al., 2002; Jin Woong Baek, et al., 2016). The method consists of digestion of fly ash samples in a mixture of HF–HNO<sub>3</sub>–HClO<sub>4</sub>–H<sub>2</sub>SO<sub>4</sub>. Around 1 gram of fly ash was put in a 250mL beaker and mixed continuously by adding 4mL of hydrofluoric acid, 5mL of hydrochloric acid, 5mL of nitric acid and 2mL of perchloric acid. Then the mixture was mixed and heated to 220 °C. The sample was then allowed to be evaporated. Thereafter, the mixture was subjected to filtration using a 1.0µm glass fiber filter paper in a 50mL round flask. After which the filtration solution was dissolved into 50mL HCl 0.1M to yield a solution to measure the total metal concentrations. An atomic absorption spectroscopy (AAS) was used to measure the entire heavy metal concentration in the acid solutions state. All these trials were conducted in triplicates and, the average value was taken.

The heavy metal concentration can be formulated as

$$\text{Heavy metal concentration (mg/kg)} = \frac{(C_a - C_b) \times V \times F}{W} \dots\dots\dots \text{Eq (2).}$$

$C_a$  = the mean concentration

$C_b$  = the concentration of metal in original sample (mg/kg)

$V$  = the volume of the digested solution made (ml)

$W$  = the dry weight of sample (g)

$F$  = the dilution factor if needed (1 = in cause of no further dilution)

#### 3.5.4 Heavy metal leaching evaluation

To understand mobility of the heavy metals from the above solidification, in this study Korean Standard Leaching Procedure (KSLP) method (Osada, Tanigaki, Takahashi, & Sakai, 2008; Son et al., 2017) were performed and the results were compared. A 30 g of uniformly grounded samples with less than 5mm particle size and a solvent with pH 5.8~6.3 using diluted HCl was separately prepared. The grained sample was mixed together using a solid to liquid ratio of 1:10 to a total volume of 50mL. The mixture was kept in a container for 6 hour at 200 rpm with 4-5 cm shaking widths. The mixture was then to subjected to a centrifuge at 3000 rpm for 20 min and filtered using a 0.45  $\mu\text{m}$  membrane filter. The heavy metals ( $\text{Cu}^{2+}$ ,  $\text{Zn}^{2+}$ ,  $\text{Pb}^{2+}$ ,  $\text{Cr}^{3+}$  and  $\text{Cd}^{2+}$ ) in the filtrate solution were analysed by atomic absorption spectroscopy (AAS) to evaluate its potential leachability. All experimental runs were done in triplicates and the averaged value was taken for the results represented in this study.

## 4. EXPERIMENTAL RESULTS AND DISCUSSION

### 4.1 Heavy metal contents and leaching concentrations

The total heavy metal content of fly ash, waste foundry sand, and GGBFS were analyzed. Table 4-1 shows the result of heavy metal contents from MBA and leaching concentration by KSLP method. The heavy metal contents of the fly ash are Zn 11,687.5mg/kg, Fe 14,575mg/kg, Cu 35mg/kg, Ni 220mg/kg and Cr 2412.5mg/kg, and Pb 46mg/kg. The theoretical maximum leaching concentration values are also tabulated. Theoretically, among the highest leaching metal concentration are Fe (291.5mg/l) and Zn (233.75mg/l) while the lowest leaching metal concentration are Cu (0.7mg/l) and Pb (0.92mg/l). Table 4-1 further shows the leaching concentration of heavy metals in the fly ash, foundry sand and GGBFS. These were measured by the KSLP method. The KSLP method presented an initial concentration of fly ash leaching concentration in the order of Fe (1.55mg/l), Pb (0.21 mg/l), Ni (0.18mg/l), Cu (0.02mg/l), Zn (0.024mg/l) and Cr (0.04mg/l). The initial heavy metal concentrations are differing in the fly ash material for MBA and KSLP due to differing acidic state. The MBA method showed higher heavy metal contents in Fe and Zn but the KSLP method indicated higher leaching metal concentration in Fe and Pb. Therefore, future studies regarding these methods are recommended. For foundry sand, the initial heavy metal concentration was measured through the KSLP method. This showed concentrations of Fe 0.19mg/l, Zn 0.014mg/l, Cu 0.018mg/l, both Cr and Ni 0.02mg/l, and Pb 0.08mg/l. Furthermore, the initial

concentration of GGBFS in all its metal concentration is substantially lower except for Fe in comparison with the other materials. In the aspect of the Korean regulatory limit, the materials after the leaching test were all below the set limitation which proves to show that this solidification method is safe for the environment. Based on the total heavy metal content of fly ash, 77-100% heavy metal concentration were immobilized. Specifically, the heavy metal immobilized efficiency is as follows: Pb 77%, Cr 99.9%, Cu 97%, Fe 99.4%, Ni 96%, and Zn 99.9%.

Table 4-1 Heavy metals content and leaching concentration of fly ash, foundry sand, and GGBFS

Materials		Pb	Cr	Cu	Fe	Ni	Zn
Fly ash (MBA) (mg/kg)	Range	(45-47.5)	(2410-2415)	(30-40)	(14500-14650)	(210-230)	(11525-11850)
	Average	46	2412.5	35	14575	220	11687.5
Theoretical Maximum Leaching (mg/l)	Range	(0.90-0.95)	(48.2-48.3)	(0.6-0.8)	((290-293)	(4.2-4.6)	(230.5-237)
	Average	0.92	48.25	0.7	291.5	4.4	233.75
Fly ash (KSLP) (mg/l)	Range	(0.18-0.24)	(0.02-0.04)	(0.021-0.03)	(1.4-17)	(0.18-0.20)	(0.03-0.045)
	Average	0.21	0.04	0.02	1.55	0.18	0.024
Foundry sand (KSLP) (mg/l)	Range	(0.07-0.1)	(0.01-0.02)	(0.015-0.022)	(0.18-0.20)	(0.02-0.02)	(0.013-0.015)
	Average	0.08	0.02	0.018	0.19	0.02	0.014
GGBFS (KSLP) (mg/l)	Range	(0.01-0.05)	(0.006-0.007)	(0.003-0.006)	(0.12-0.15)	(0.025-0.03)	(0.014-0.018)
	Average	0.03	0.007	0.004	0.135	0.031	0.016
Korean regulatory limit:		3.0	1.5	1.0	-	-	3.0

Table 4-2 and Fig. 4-1 show the GPC solidification of the 14 runs after heavy metals leaching concentration under the KSLP method in different mixing ratios of foundry sand, fly ash and GGBFS. In GPC, the average heavy metals leaching concentration is Cu 0.014mg/l, Cr 0.013mg/l, Pb 0.019mg/l, Zn 0.02mg/l, Fe 0.06mg/l and Ni 0.067mg/l. These heavy metals leaching result are also well within the Korean regulatory limit. Moreover, the heavy metals concentration in the mixture of fly ash, foundry sand and GGBFS materials has the highest leaching capacity in the order of Cu and Cr > Pb > Zn > Fe > Ni. The highest leaching concentration in Pb is R2 (0.2mg/l), this is attributed to a higher content of foundry sand which leads towards low leaching results in Pb. The lowest leaching concentration in Pb is in R10 (0.17mg/l) this is due to a higher foundry sand mixture ratio. Moreover, Cr has the highest leaching concentration in R1, R2, R5, R6, and R12 of 0.02mg/l and all other runs has a low concentration of 0.01mg/l. A low Cr leaching outcome is observed when the fly ash gets lower and foundry sand gets higher. The Cu leaching result in R4, R5 and R13 have the highest leaching concentration due to more foundry sand and less fly ash ratios. On the other hand, the fly ash ratio is lower in the leaching of Fe as seen in R4 and R9 (0.5mg/l). Ni has the lowest leaching concentration in R7, R9, and R14. When the fly ash ratio gets lower and foundry sand get higher, the Ni leaching concentration is reduced. Furthermore, when the foundry sand and fly ratio is in the average interval, the Zn leaching concentration get decreased as seen in R7 and R13. Based on the overall results, the increase in foundry sand ratio decreases the heavy metals leaching concentration. This is due to the presence of silica in foundry sand as reported in Siddique & Noumowe (2008). A higher foundry sand ratio gives more silica

content that aids heavy metals immobilization (Rao & Liu, 2015). In the GPC specimen, the achieved heavy metals immobilization ranges from 92.1 to 99.98% which is promising for environmental applications based on the total heavy metals content of fly ash. Specifically, after the GPC solidification, the heavy metals immobilized percentages were Pb 93.3 – 95.9%, Cr 99.8-99.9%, Cu 92.1-96.6%, Fe 99.3-99.5%, Ni 95.7-96.8% and Zn 99.97-99.98%. Based on the overall results of the heavy metals leaching, the addition of GGBFS with foundry sand and fly ash can potentially reduce heavy metals leaching from the concrete in any ratios.

**Table 4-2** KSLP Leaching concentration of heavy metal in different mixing ratios

<b>Run FS/FA/GGBFS%</b>		<b>Pb (mg/l)</b>	<b>Cr (mg/l)</b>	<b>Cu (mg/l)</b>	<b>Fe (mg/l)</b>	<b>Ni (mg/l)</b>	<b>Zn (mg/l)</b>
<b>Run1 25.3/50. 6/24.0</b>	<b>Range</b>	(0.015- 0.023)	(0.016- 0.024)	(0.01- 0.014)	(0.67- 0.73)	(0.07- 0.09)	(0.018- 0.022)
	<b>Average</b>	0.019	0.02	0.012	0.7	0.08	0.02
<b>Run2 25.3/50. 6/24.0</b>	<b>Range</b>	(0.012- 0.028)	(0.017- 0.023)	(0.011- 0.013)	(0.6- 0.8)	(0.072- 0.088)	(0.018- 0.022)
	<b>Average</b>	0.02	0.02	0.012	0.7	0.08	0.02
<b>Run3 44.0/37. 4/18.6</b>	<b>Range</b>	(0.015- 0.025)	(0.007- 0.013)	(0.011- 0.017)	(0.68- 0.72)	(0.065- 0.075)	(0.017- 0.019)
	<b>Average</b>	0.02	0.01	0.014	0.7	0.07	0.018
<b>Run4 45.8/32. 8/21.4</b>	<b>Range</b>	(0.014- 0.026)	(0.005- 0.015)	(0.014- 0.022)	(0.42- 0.58)	(0.052- 0.068)	(0.017- 0.023)
	<b>Average</b>	0.02	0.01	0.018	0.5	0.06	0.02
<b>Run5 47.3/35. 7/17.0</b>	<b>Range</b>	(0.011- 0.029)	(0.015- 0.025)	(0.012- 0.022)	(0.4-0.7)	(0.08- 0.1)	(0.018- 0.022)

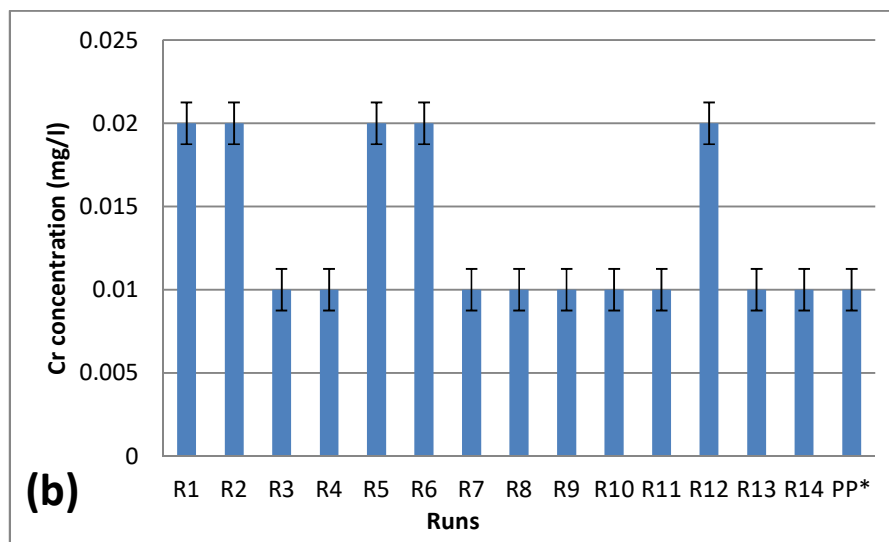
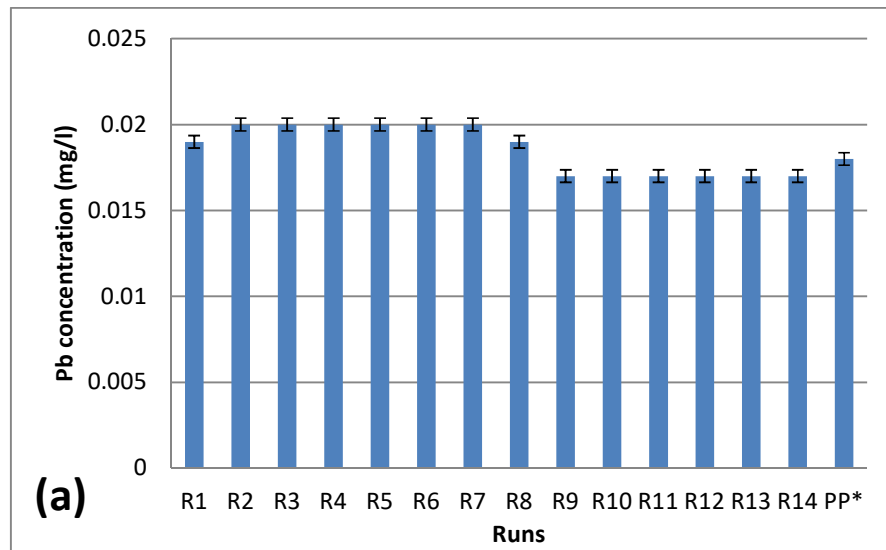


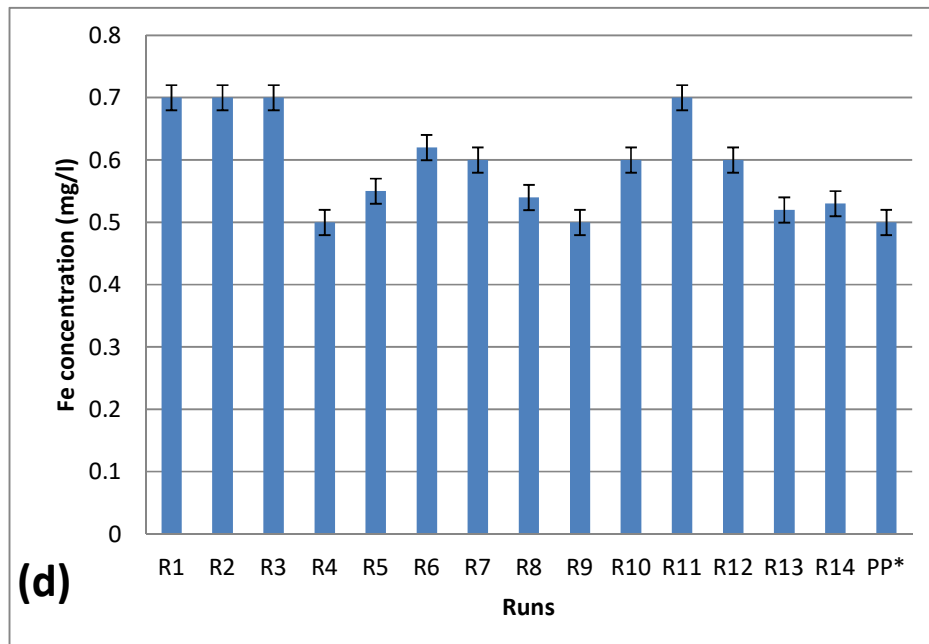
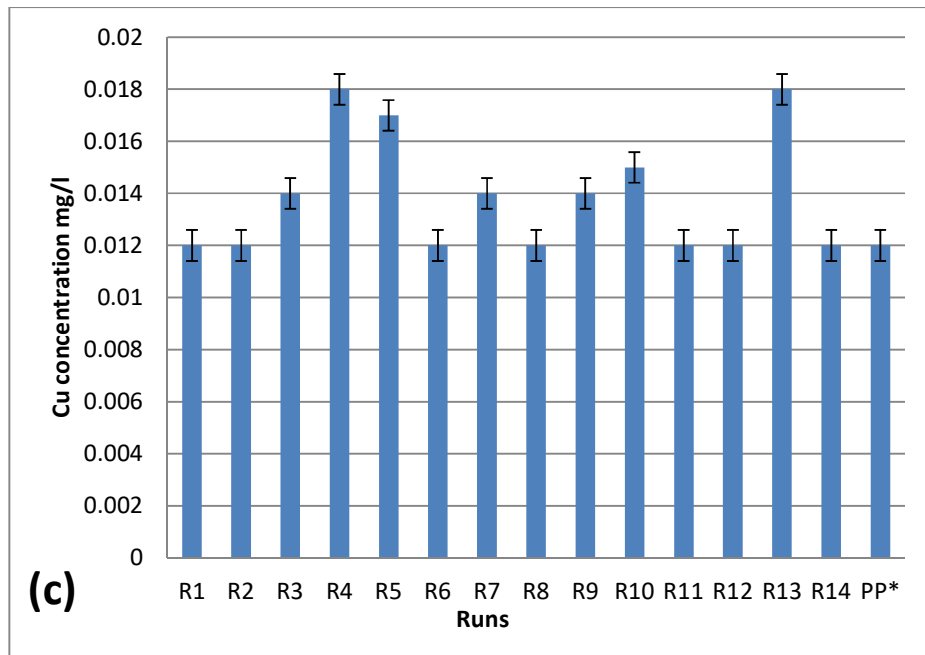
	<b>Average</b>	0.02	0.02	0.017	0.55	0.09	0.02
<b>Run6 38.3/41. 8/19.9</b>	<b>Range</b>	(0.016- 0.024)	(0.017- 0.023)	(0.007- 0.017)	(0.47- 0.77)	(0.079- 0.081)	(0.017- 0.023)
	<b>Average</b>	0.02	0.02	0.012	0.62	0.08	0.02
<b>Run7 39.3/36. 6/24.0</b>	<b>Range</b>	(0.012- 0.028)	(0.008- 0.012)	(0.011- 0.017)	(0.43- 0.77)	(0.047- 0.053)	(0.009- 0.011)
	<b>Average</b>	0.02	0.01	0.014	0.6	0.05	0.01
<b>Run8 50.3/31. 7/17.9</b>	<b>Range</b>	(0.017- 0.021)	(0.007- 0.013)	(0.011- 0.013)	(0.3- 0.78)	(0.052- 0.068)	(0.014- 0.026)
	<b>Average</b>	0.019	0.01	0.012	0.54	0.06	0.02
<b>Run9 52.9/27. 5/19.6</b>	<b>Range</b>	(0.14- 0.02)	(0.009- 0.011)	(0.013- 0.015)	(0.49- 0.51)	(0.043- 0.057)	(0.014- 0.018)
	<b>Average</b>	0.017	0.01	0.014	0.5	0.05	0.016
<b>Run10 46.4/33. 7/19.9</b>	<b>Range</b>	(0.01- 0.024)	(0.006- 0.014)	(0.014- 0.016)	(0.52- 0.68)	(0.05- 0.07)	(0.012- 0.022)
	<b>Average</b>	0.017	0.01	0.015	0.6	0.06	0.017
<b>Run11 37.3/40. 9/21.8</b>	<b>Range</b>	(0.013- 0.021)	(0.008- 0.012)	(0.01- 0.014)	(0.65- 0.75)	(0.068- 0.072)	(0.014- 0.024)
	<b>Average</b>	0.017	0.01	0.012	0.7	0.07	0.019
<b>Run12 47.3/35. 7/17.0</b>	<b>Range</b>	(0.012- 0.022)	(0.018- 0.022)	(0.01- 0.014)	(0.57- 0.63)	(0.089- 0.091)	(0.013- 0.017)
	<b>Average</b>	0.017	0.02	0.012	0.6	0.09	0.015
<b>Run13 39.3/36. 6/24.0</b>	<b>Range</b>	(0.014- 0.02)	(0.009- 0.011)	(0.014- 0.022)	(0.48- 0.56)	0.042- 0.058)	(0.009- 0.011)
	<b>Average</b>	0.017	0.01	0.018	0.52	0.05	0.01
<b>Run14 52.9/27. 5/19.6</b>	<b>Range</b>	(0.015- 0.019)	(0.008- 0.012)	(0.011- 0.013)	(0.46- 0.6)	(0.035- 0.045)	(0.011- 0.019)
	<b>Average</b>	0.017	0.01	0.012	0.53	0.04	0.015

<b>Run</b>	<b>Range</b>	(0.016-0.02)	(0.008-0.012)	(0.01-0.014)	(0.47-0.53)	(0.066-0.074)	(0.015-0.019)
<b>*PP</b>	<b>Average</b>	0.018	0.01	0.012	0.5	0.07	0.017
<b>39.8/37.4/22.9</b>							
<b>Average</b>		0.019	0.013	0.014	0.06	0.067	0.02

*\*PP – Point Prediction,*

*\*FS- Foundry sand, \*FA- Fly Ash*





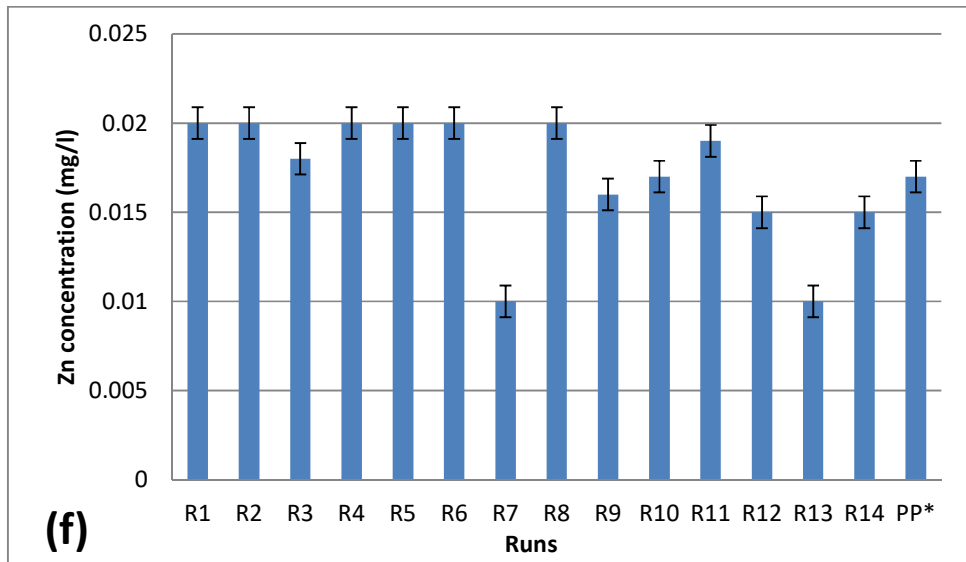
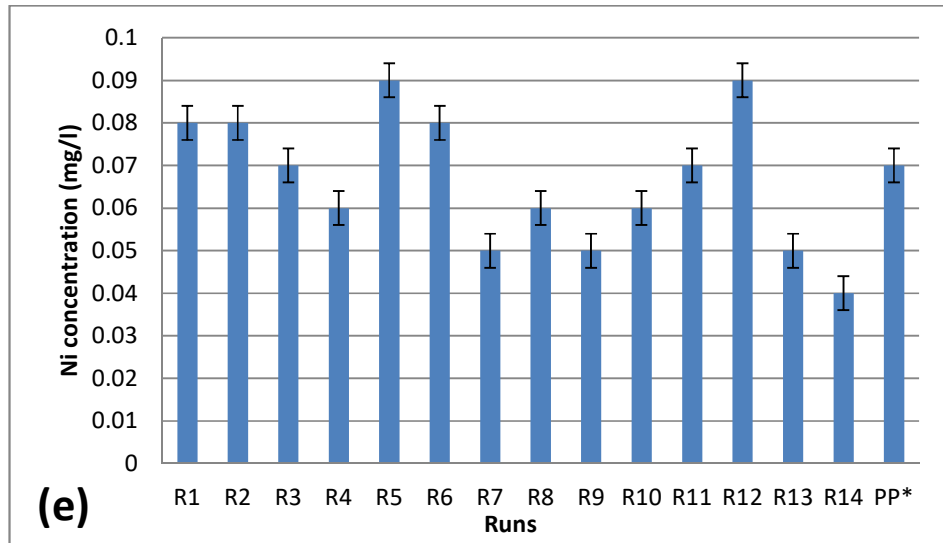


**Figure 4-1** Heavy metal leaching for (a) Pb, (b) Cr, (c) Cu, (d) Fe, (e) Ni and (f) Zn

## 4.2 Compressive strength

In this study, for GPC fly ash, GGBFS, fine aggregate, waste foundry sand, coarse aggregate, and alkaline solution are mixed to be a specimen was casted. Compressive strength of the specimen compared is tabulated in the experimental results. Here GGBFS, coarse aggregate and alkaline solution mixing ratio is constant. For the remaining materials fly ash, waste foundry sand, and the sand ratio design export software is used and optimum mix design is prepared.

Table 4-3 shows the compressive strength result. From the table, it can be observed that the actual compressive strength of 7<sup>th</sup> and 28<sup>th</sup> day is maximum at 18.6Mpa and 22Mpa when 51.9wt% fine aggregate, 24.8wt% WFS and 23.3wt% fly ash is used. The predicted strengths of the specimen for this composite using the D-optimal mixture design are 19.0Mpa and 22.2Mpa respectively which are in close approximate of the actual values.

The result R1, R2, R7, R9, R10, R13 and \*PP were at higher compressive strength compared to the conventional concrete. It can be observed when the sand ratio is higher and fly ash ratio is higher, compressive strength is higher (R1 and R2). When the sand ratio is higher, waste foundry sand ratio is average and fly ash ratio is lower, compressive strength value is higher (R7 and R13). But if the sand ratio is lower, fly ash and waste foundry sand ratio is increased; compressive strength has shown to be very low strength.

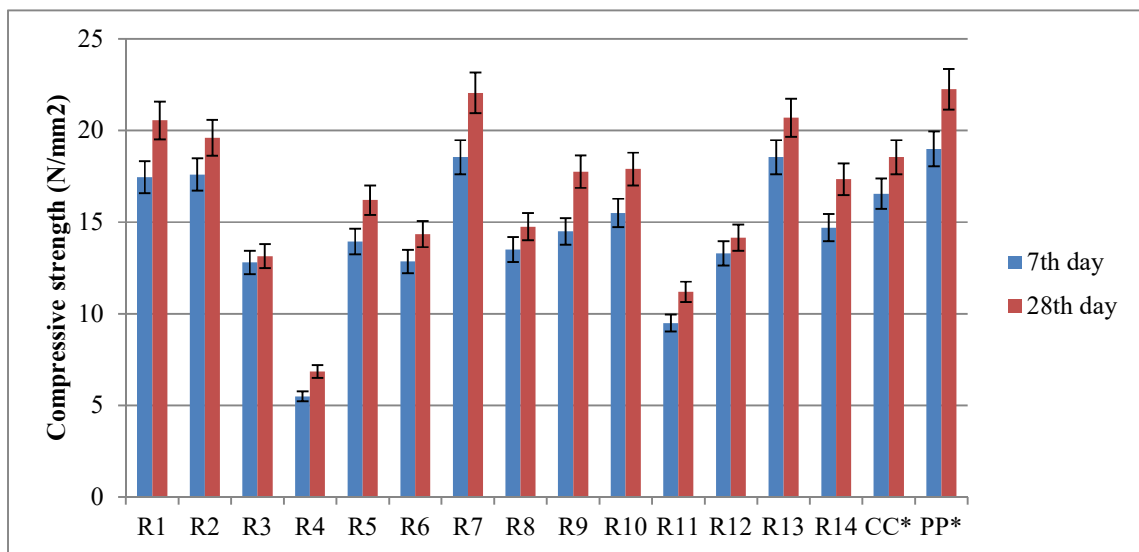
**Table 4-3** Compressive strength of specimen for various tests and the conventional concrete

Run Test FA/FS/fly ash%	Compressive strength (MPa)			
	7 <sup>th</sup> day		28 <sup>th</sup> day	
	Range	Average	Range	Average
<b>R1</b> <b>55/15/30</b>	16.4-18.5	17.4	19.9-21.2	20.5
<b>R2</b> <b>55/15/30</b>	16.3-8.9	17.6	18.9-20.3	19.6
<b>R3</b> <b>37.8/33.6/28.6</b>	10.0-15.6	12.8	12.4-13.9	13.1
<b>R4</b> <b>47.7/30.5/21.8</b>	5.30-5.70	5.5	6.3-7.4	6.8
<b>R5</b> <b>30.3/39.7/30</b>	13.5-14.4	13.9	15.1-17.3	16.2
<b>R6</b> <b>42.5/27.5/30</b>	11.6-14.1	12.8	13.8-14.9	14.3
<b>R7</b> <b>55/23.3/21.7</b>	18.0-19.1	18.5	21.4-22.7	22.05
<b>R8</b> <b>34.8/40/25.2</b>	12.4-14.6	13.5	14.1-15.4	14.7
<b>R9</b> <b>41.5/38.5/20</b>	13.6-15.4	14.5	16.9-18.6	17.7
<b>R10</b> <b>42.5/33.3/24.2</b>	15.1-15.9	15.5	17.3-18.5	17.9
<b>R11</b> <b>48.9/24.4/26.7</b>	9.30-9.70	9.5	10.0-12.4	11.2
<b>R12</b> <b>30.3/39.7/30</b>	13.0-13.6	13.3	13.2-15.1	14.1
<b>R13</b> <b>55/23.3/21.7</b>	17.4-19.7	18.5	19.9-21.5	20.7
<b>R14</b> <b>41.5/38.5/20</b>	14.3-15.1	14.7	16.3-18.4	17.3
<b>PP*</b> <b>51.9/24.8/23.3</b>	18.7-19.3	19.0	21.3-23.2	22.2
<b>CC*</b>	16.3-16.8	16.5	18.0-19.1	18.5

*\*cc – Conventional Concrete, \*PP – Point Prediction*

*\*FA- Fine Aggregate, \*FS- Foundry Sand*

Figure 4.2 shows the compressive strength variation in foundry sand based GPC and conventional concrete. The minimum compressive strength GPC is R4 5.5Mpa (7<sup>th</sup> day) and 6.8Mpa (28<sup>th</sup> day) and maximum compressive strength is 19.0Mpa (7<sup>th</sup> day) and 22.2Mpa (28<sup>th</sup> day), but conventional concrete strength is 16.5Mpa (7<sup>th</sup> day) and 18.5Mpa (28<sup>th</sup> day).The conventional concrete strength is lower than compared to GPC, because of waste foundry san, fly ash and alkaline solution. The waste foundry sand, fly ash and alkaline solution have more silica content, so they silica property cause is increase the strength of concrete. If add more foundry sand and fly ash that time compressive strength gets decreased, because silica property get more and CaO get decreased.

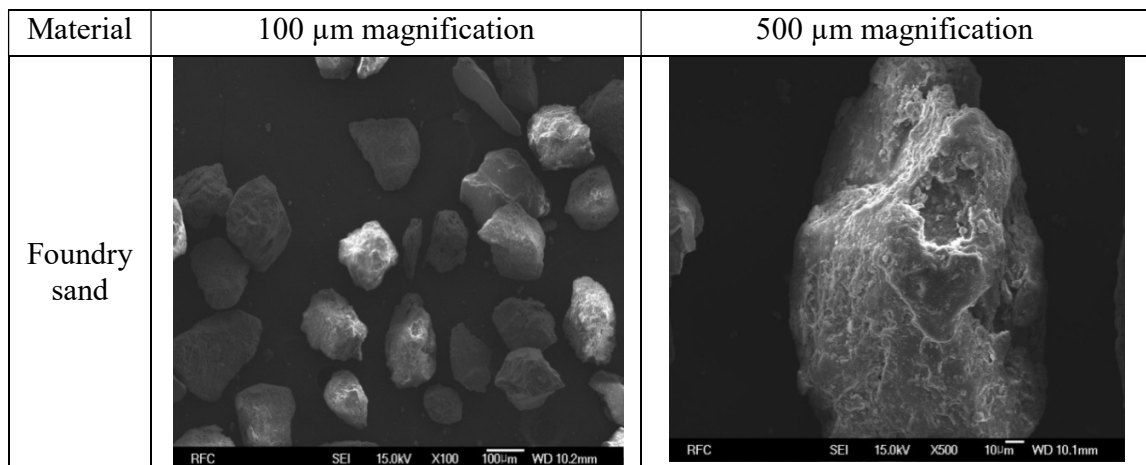


\*cc – Conventional Concrete, \*PP – Point Prediction

**Figure 4-2** Compressive strength with compression of 7<sup>th</sup> and 28<sup>th</sup> day

### 4.3 FE-SEM & XRD analysis

To examine whether heavy metals leached are contained in the fly ash and suppressed when the materials are used as construction material, the FE-SEM/EDS analysis is used. The images in Fig 4.3 illustrate the FE-SEM of the waste foundry sand, fly ash, GGBFS and R7 (GPC after solidification). The particle size distribution has been significantly reduced which can be observed in the images. Moreover, homogeneous sets of particles are formed after foundry sand solidification. For the crystal form analysis, the specimens were solidified in air for one day and then observed at 100 and 500 $\mu$ m magnification through FE-SEM / EDS. The analyzed crystal form photographs analyzed are shown individually in Fig. 4.3.





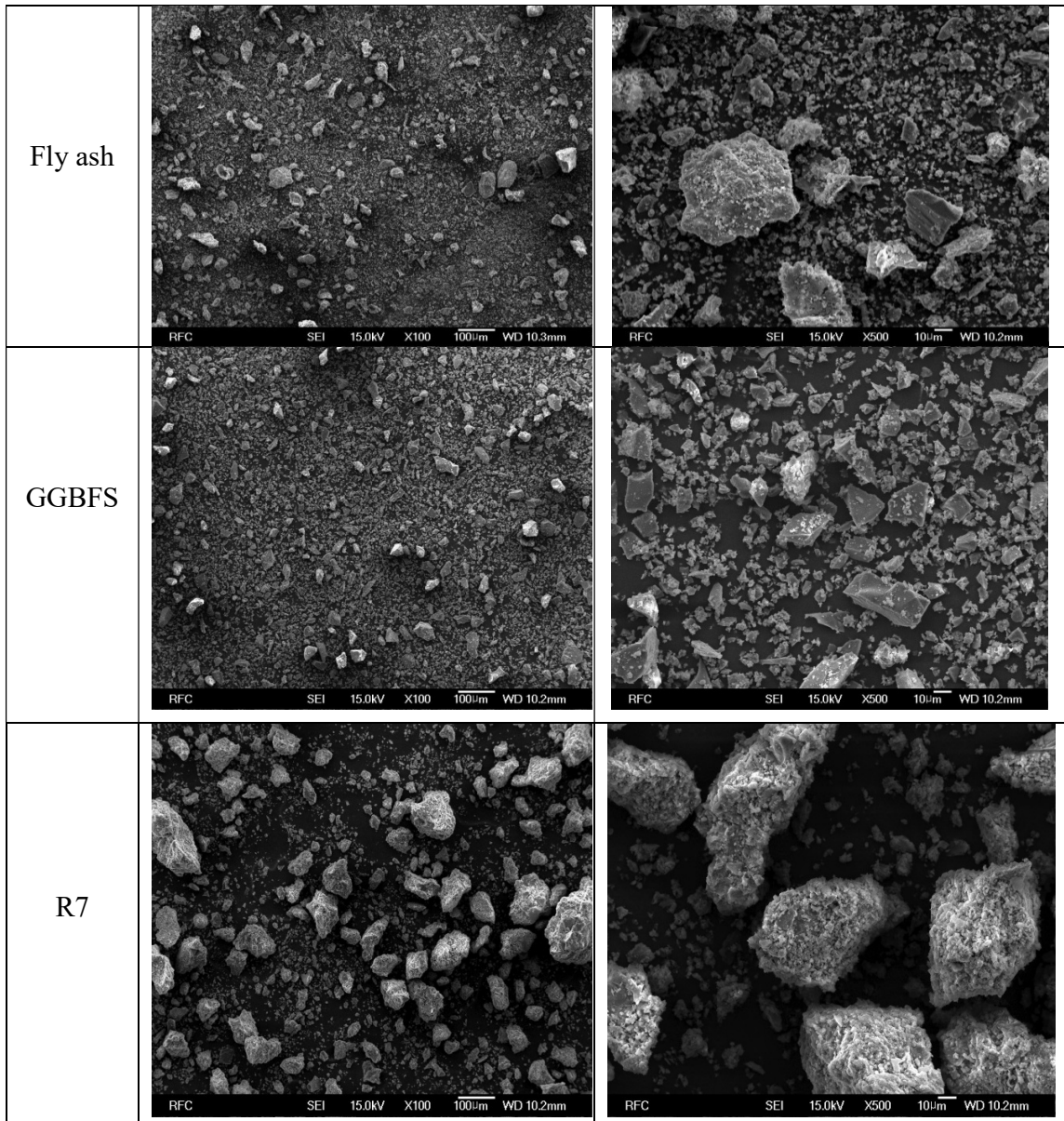


**Figure 4-3** FE-SEM images

Through the XRD analysis, it is observed that the composite and pattern of ash containing lot of harmful substances are immobilized. Therefore, the reuse and recycling of fly ash materials can be encouraged in construction materials. The corresponding

representative components and patterns before and after solidification are shown in Fig.4.4 and 4.5

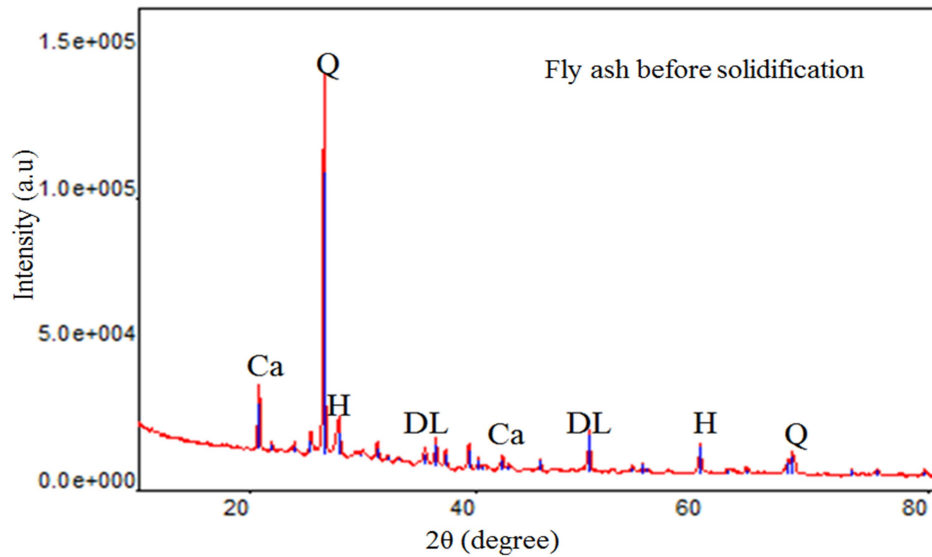
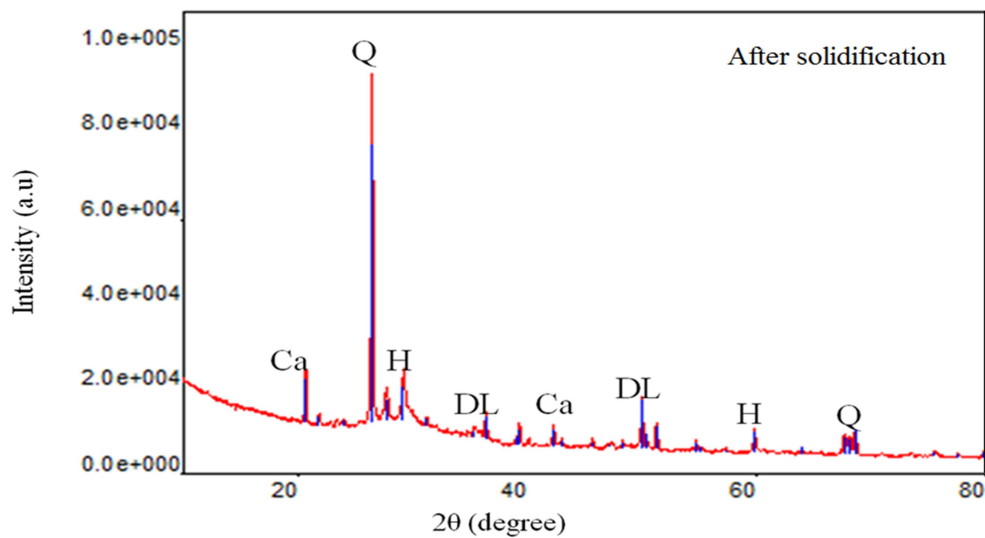


Figure 4-4 XRD analysis to determine the patterns before solidification



*Q: Quartz, Ca: Calcite, DL: Dolomite, H: Hematite*

Figure 4-5 XRD analysis to determine the patterns after solidification

The major constituents of the fly ash material (before use) majorly comprise of quartz ( $\text{SiO}_2$ ), in addition to other minor constituents such as calcium oxide ( $\text{CaCO}_3$ ), hematite ( $\text{Fe}_2\text{O}_3$ ), aluminum oxide hydrate ( $5\text{Al}_2\text{O}_3\text{-H}_2\text{O}$ ), dolomite ( $\text{CaMg}(\text{CO}_3)_2$ ), calcium silicate hydrate ( $\text{Ca}_{1.5}\text{SiO}_{3.5}\text{nH}_2\text{O}$ ), and calcium aluminate hydrate ( $\text{Ca}_3\text{Al}_2\text{O}_6\text{nH}_2\text{O}$ ) (Swanson & Tatge, 1951). When most of the fly ash is crystallized in the form of the hydrate, all the aforementioned metals have been converted to sulfides/sulfites. Therefore, by mixing with GPC, solidification of heavy metal compounds is presumed to be caused by metal hydroxide formed by chemical reaction. As a result, it seems that coagulation of harmful substances (heavy metals) of fly ash is effective.

#### **4.4 Response surface optimization**

The optimized provisions of the GPC solidification method the highest compressive strength were achieved and concurrent solving the regression equation and analysis the response surface plots. The method of verifying the authenticity and truth of the model ensured the runs were the use of suitable conditions.

The predicted compressive strength result of this test indicates that the computational interval values are a good compromise because the quadratic model is efficient and optimistic indicates that progress is adequate.

The quadratic model was used to relate preliminary data and getting the recession equations. The resolve of the response constant ( $\beta_i$  and  $\beta_{ij}$ ) aimed at the self-governing variables (A, B and C) is made using test data. Equation 3&4 show the compressive

strength in GPC solidification of the response surface predictive model. Using the quadratic model the regression equation is obtained by correlating the preliminary data.

The response coefficients ( $\beta_i$  and  $\beta_{ij}$ ) for the independent Variables (A, B and C) were determined by using the preliminary data. Equation 3 and 4 represent the response surface predictive model of the GPC solidification compressive strength (Y).

$$Y_{7^{\text{th}} \text{ day CS}} = 12.31A + 17.60B - 1661.95C - 8.31AB + 3193.06AC + 2879.15BC - 3325.75ABC + 112.13AB(A-B) - 1087.47AC(A-C) - 1077.72BC(B-C) \dots \dots \dots \text{Eq(3)}$$

$$Y_{28^{\text{th}} \text{ day CS}} = 13.60A + 19.88B - 1920.44C - 9.04AB + 3696.78AC + 3327.88BC - 3844.63ABC + 136.34AB(A-B) - 2099.68AC(A-C) - 1241.53BC(B-C) \dots \dots \dots \text{Eq(4)}$$

#### 4.5 Statistical results

Table 4.4& 4.5 summarizes the results of the ANOVA for the compressive strength of the specimen in GPC solidification on 7<sup>th</sup> day and 28<sup>th</sup> day respectively. The level of reliance is assumed to be 0.05 to examine the response of the surface quadratic model. The result of the integration of the process and parameters are determined using Fisher variant ratio (F-value) and calculated probability (p-value). A smaller p-value (<0.05) demonstrate that the resultant independent variable is statistically meaningful. Moreover, high F-value (160.33 and 28.95 for 7<sup>th</sup> and 28<sup>th</sup> day respectively) illustrates the variance of average data can be explained by the variables in the quadratic form equation (Bilici Baskan & Pala, 2010; Choi, et al., 2017; Subramonia et al., 2017). It can be observed from the F-value and p-value, that the generated quadratic model is statistically significant.

**Table 4-4** Statistical analysis of compressive strength in solidified GPC on 7<sup>th</sup> day

Source	Sum of squares	Degrees of freedom	Mean Square	F-value	p-value	Results
Model	167.74	9	18.64	160.33	<0.0001	Significant
Linear mixture	23.16	2	11.58	99.62	0.0004	
AB	3.36	1	3.36	28.95	0.0058	
AC	39.69	1	39.69	341.42	<0.0001	
BC	38.46	1	38.46	330.84	<0.0001	
ABC	41.66	1	41.66	358.34	<0.0001	
AB(A-B)	60.15	1	60.15	517.40	<0.0001	
AC(A-C)	39.90	1	39.90	343.19	<0.0001	
BC(B-C)	30.96	1	30.96	266.34	<0.0001	
Pure Error	0.46	4	0.12			
Cor total	168.21	13				

R<sup>2</sup>=0.9972    Adj-R<sup>2</sup>=0.9910    Adeq precision=45.1    C.V.%=2.42

**Table 4-5** Statistical analysis of compressive strength in solidified GPC on 28<sup>th</sup> day

Source	Sum of squares	Degrees of freedom	Mean Square	F-value	p-value	Results
Model	217.87	9	24.21	29.93	0.0026	Significant
Linear mixture	36.12	2	18.06	22.33	0.0068	
AB	3.98	1	3.98	4.93	0.0907	
AC	53.20	1	53.20	65.78	0.0013	
BC	51.38	1	51.38	63.53	0.0013	
ABC	55.67	1	55.67	68.83	0.0012	
AB(A-B)	74.96	1	74.96	92.68	0.0007	
AC(A-C)	53.84	1	53.84	66.57	0.0012	
BC(B-C)	41.09	1	41.09	50.81	0.0020	
Pure Error	3.24	4	0.81			
Cor total	221.10	13				

R<sup>2</sup>=0.9854    Adj-R<sup>2</sup>=0.9524    Adeq precision=19.3    C.V. %=5.56

On 7<sup>th</sup> and 28<sup>th</sup> day, the interactive terms of AB, AC and BC were significant in the compressive strength in solidification of GPC. It can be observed that the 7<sup>th</sup> and 28<sup>th</sup> day F-values (29.93, 4.93) are small and p-values (0.0053, 0.0978) are high. These values

imply that no significance is relative to lack of fit pure error in quadratic model. In the mathematical model, the usually reliable fit is based on the coefficient of the drive ( $R^2$ ). The adjusted coefficient of the drive (Adj- $R^2$ ) is generally used to define the important fit quality. High Adj- $R^2$  of 0.9910, 0.9524 for both compressive strengths respectively confirmed that the generated cubic model can determine the precise range of tested model and has a good fit.

This indicates that some adequacy from the model can be employed in optimizing its corresponding responses. The signal to noise ratio identifies the adequacy of the signal can be observed at every value of the adequate precision. The variance in the predicted response is measured based on the accompanying error. The value 4 for the ratio indicate that the signal is satisfactory (Choi et al., 2014; Sengupta, 2014). Consequently, they acquired ratio of 7<sup>th</sup> and 28<sup>th</sup> day compressive strength (45.304, and 18.945) for the Adeq accuracy in the quadratic model imply sufficient signal to steer the design space. The mark of precision, where strategies are associated, is assessed by the coefficient of variation (C.V. %). For low C.V. % value the experiments are determined to be highly reliable (Muteki et al., 2007; Li et al., 2009). Therefore, the C.V. % of 2.42, and 5.56 determined based on the compressive strength. Based on the quadratic model formed, Fig. 4-6, 4-7, 4-8, and 4-9 demonstrates the characteristic plots from the GPC solidification process. It can be seen that 7<sup>th</sup> and 28<sup>th</sup> day compressive strengths are high based on Fig. 4-6 and 4-7, and it imply that they are stable and great fit in the design. In Fig. 4-8, and 4-9, the inside residuals exhibited that the data points which are near to normal line have an adequate fit for the model. There is no obvious problem with response change.

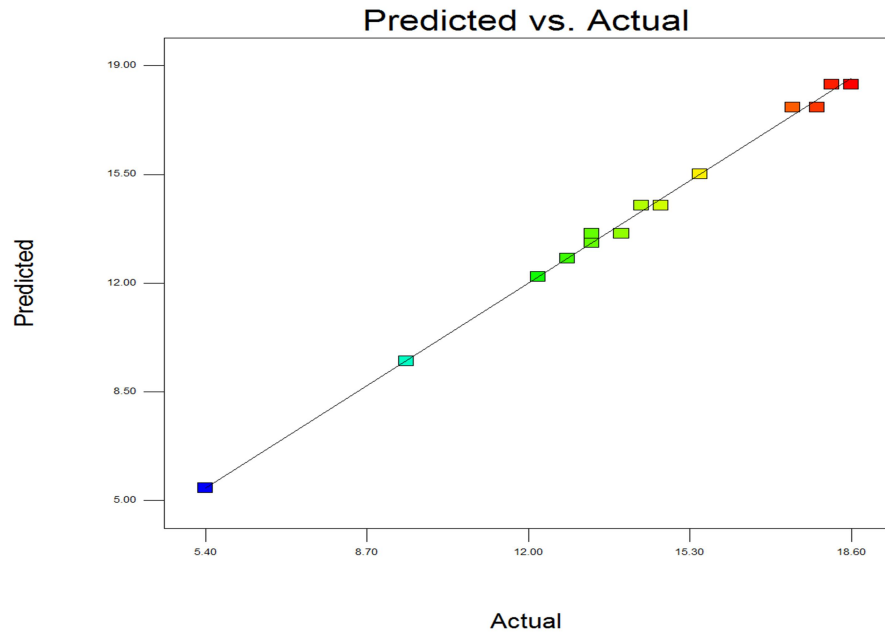


Figure 4-6 represents the 7<sup>th</sup> day predicted VS actual compressive strength values

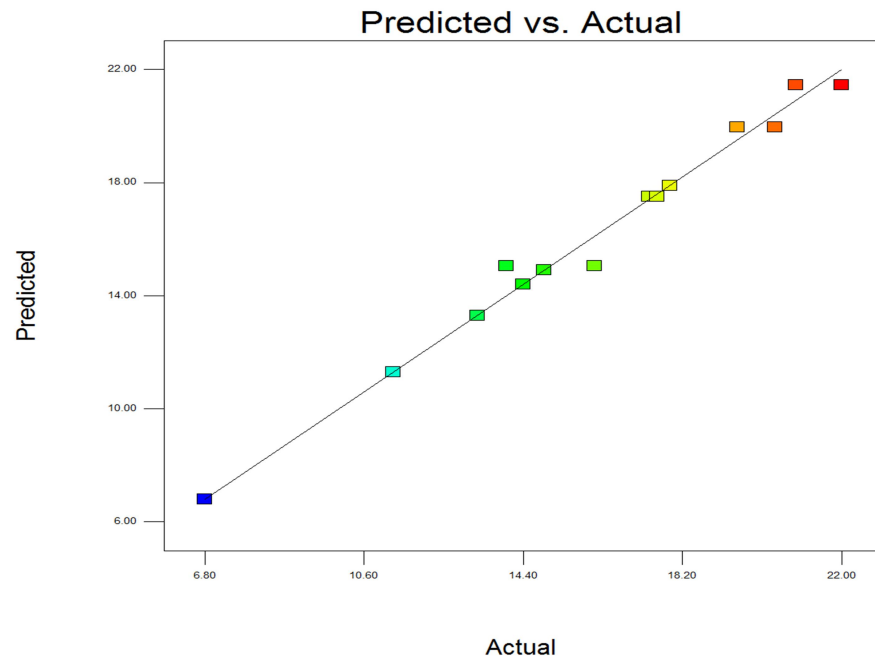
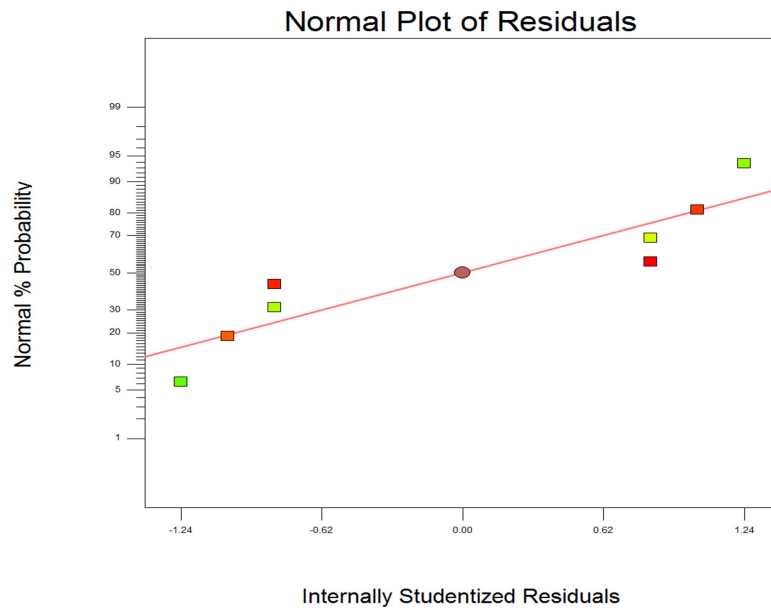
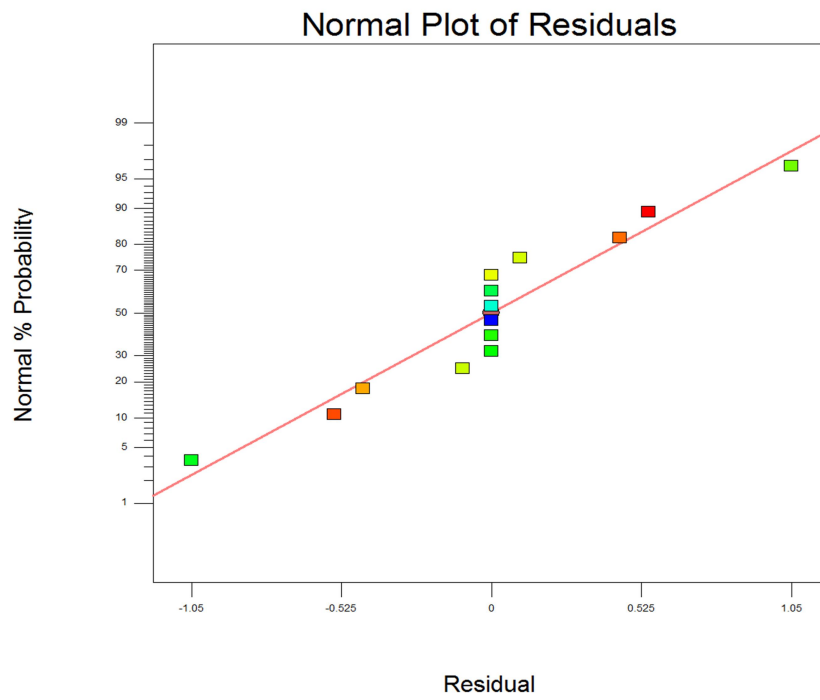


Figure 4-7 represent 28<sup>th</sup> day predicted VS actual compressive strength values



**Figure 4-8** 7<sup>th</sup> day normal plot of residuals



**Figure 4-9** 28<sup>th</sup> day normal plot of residuals



#### 4.6 Analysis of responses

Contour and 3-D plots are based response surface methodology (RSM), which is employed to investigate the effect of fine aggregate, waste foundry sand and fly ash on the compressive strength in GPC solidification. In terms of the ANOVA from the Table 4-4 and 4-5, 7<sup>th</sup> and 28<sup>th</sup> day interaction of fine aggregate towards waste foundry sand (7<sup>th</sup> day p-value=0.0058 & 28<sup>th</sup> day p-value= 0.0907) and fly ash (7<sup>th</sup> day p-value<0.0001 and 28<sup>th</sup> day p-value = 0.0013) were determined to have a substantial impact on compressive strength. The interaction of waste foundry sand and fly ash (7<sup>th</sup> day p-value<0.001 and 28<sup>th</sup> day p-value= 0.0013) produce the least impact on the response Fig 4-14 and Fig 4-15 are surface response plots and results of the two component mixtures of GPC solidification. This consistently demonstrates the important interactive consequences of fine aggregate, waste foundry sand and fly ash. Therefore, final serviceability and quality of the solidified product entirely depend on the mixing and proportioning of fine aggregate, waste foundry sand and fly ash in terms of compressive strength. The reflection of the waste foundry sand with fly ash and GGBFS in alkaline solution help to enhance the efficiency and stability of the mixture as it acts as a complementary product to improve the strength of the substance. It also illustrates that the compressive strength is directly proportional to alkaline content. Moreover, this tendency is replaced by sodium hydroxide and sodium silicate in the GPC and coordinates and controls the efficient integration of the solid material.

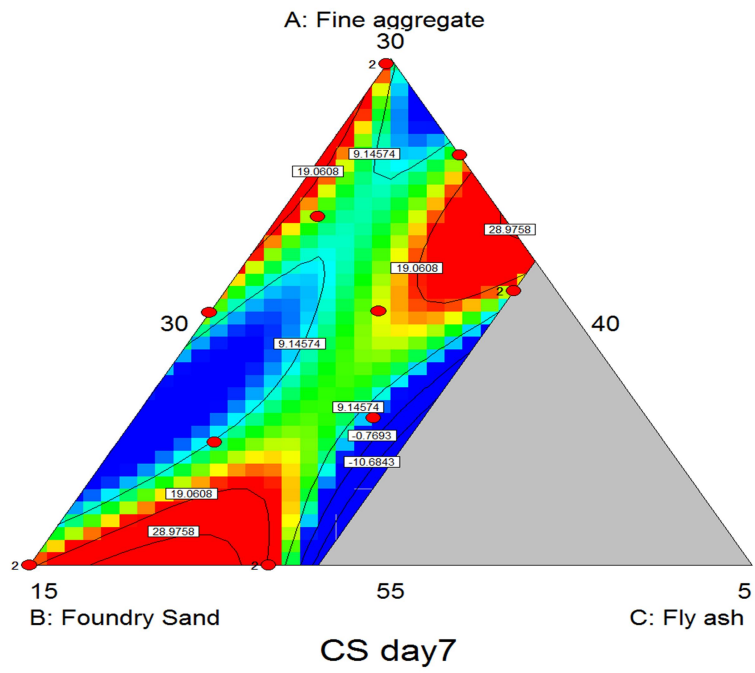


Figure 4-10 7<sup>th</sup> day contour plot

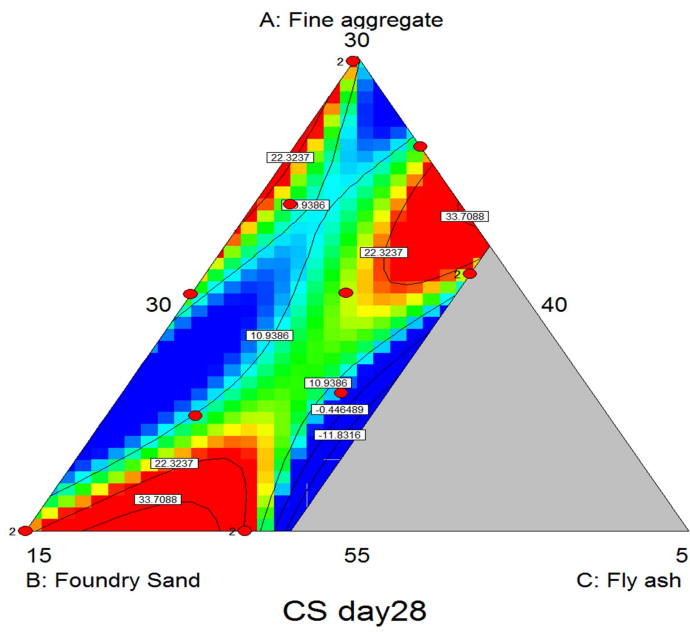
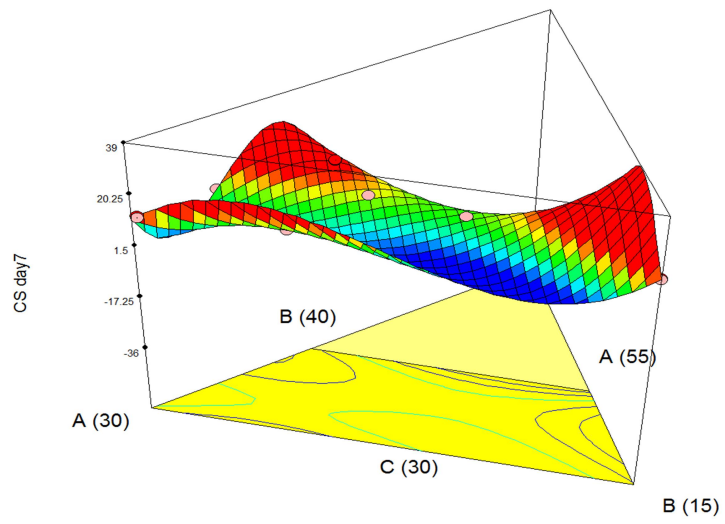
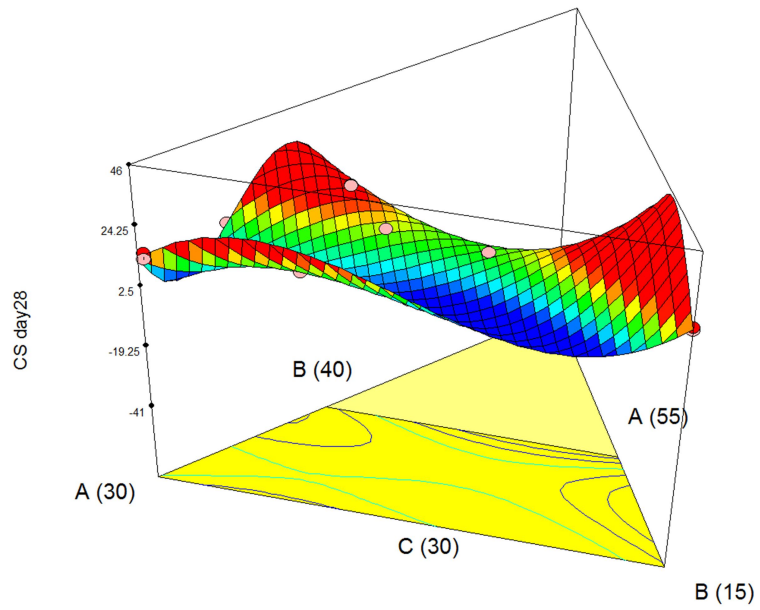


Figure 4-11 28<sup>th</sup> day contour plot



**Figure 4-12** 7<sup>th</sup> day response surface plot



**Figure 4-13** 28<sup>th</sup> day response surface plot

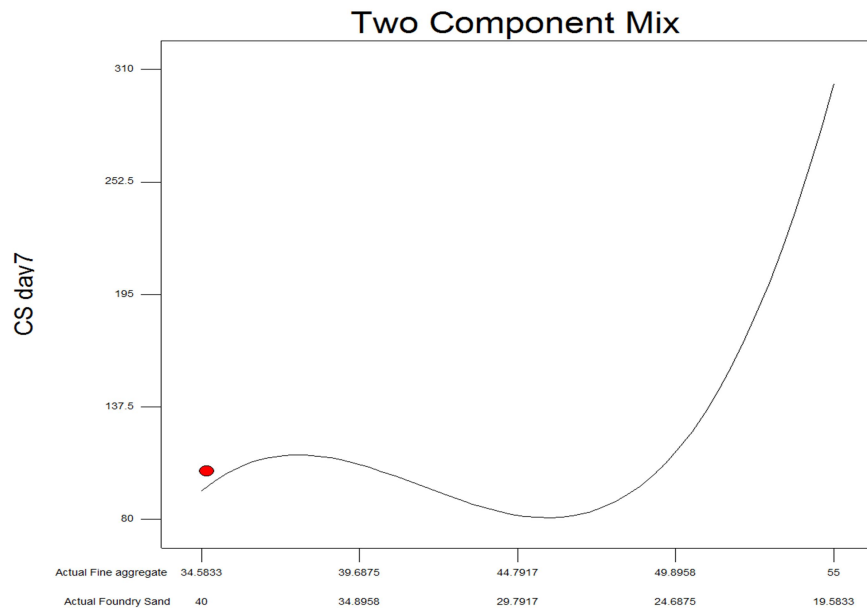


**Figure 4-14** 7<sup>th</sup> day fine aggregate and foundry sand component graph

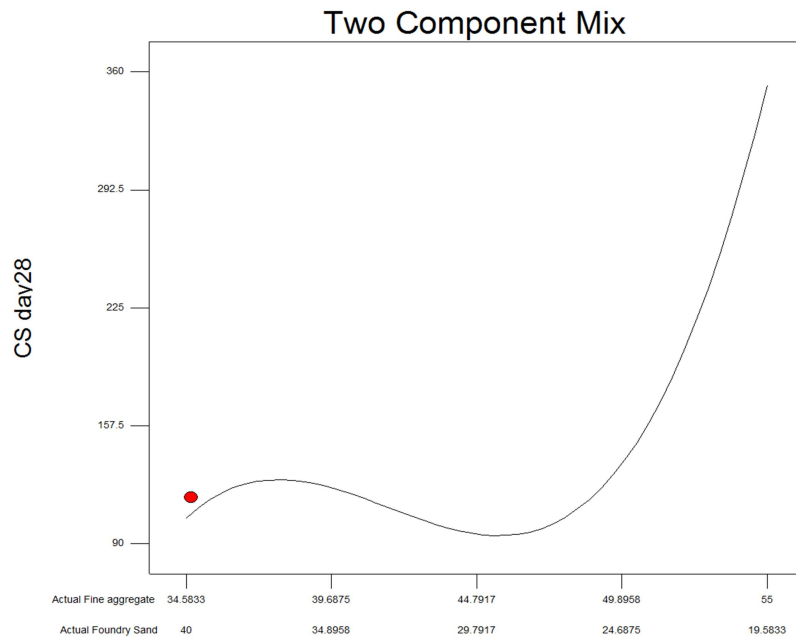


**Figure 4-15** 28<sup>th</sup> day fine aggregate and foundry sand component graph

#### **4.7 Implication of the results**

The results of heavy metals leaching of cured GPC were compared to that of Portland cement in past researches at various concrete mixtures listed in Table 4-6 (Cohen, Cilliers, & Petrie, 1997; Mangialardi et al., 1999; Son). Although the heavy metal leaching in GPC of this study did not achieve the lowest leaching results as compared in previous literatures, the results of this study have still satisfied the Korean standard leaching regulatory limit. Therefore, the use of foundry sand based GPC will not cause an environmental hazard. Moreover, as shown in Table 4-6, the compressive strength of this study is lower than the results in previous studies (Torres et al., 2017; Aggarwal & Siddique, 2014; Kurama & Kaya, 2008; Siddique, Singh, Belarbi, Ait-Mokhtar, & Kunal, 2015). This is due to past works having different materials, mixture design and concrete specimen. This research work utilizes a cylindrical specimen, but past researches used a cube specimen. The cube specimen has compressive strength higher than that of a cylindrical specimen. At optimum conditions of this study, waste foundry sand ratio of 24.8% and fly ash ratio of 23.3% showed high compressive strength. But if the sand ratio is further decreased, while fly ash and waste foundry sand ratio is further increased; the compressive strength decreases. The utilization of foundry sand in GPC can therefore influence its compressive strength. Furthermore, the foundry sand based GPC showed better performance as compared to the foundry sand based OPC in this study by 15.8 – 21.1%. This is due to the alkaline solution; fly ash and foundry sand have higher silica content.

**Table 4-6** Comparison of heavy metal leaching and compressive strength research finding in cured concrete

<b>Comparison of heavy metal leaching</b>						
	In this study	(Cohen et al., 1997)	(Mangialardi et al., 1999)	(Son et al., 2017)	(Baek et al., 2017)	Korean regulatory limit:
<b>Method</b>	Korean standard leaching method	Toxicity characteristic leaching procedure (TCLP)	Standard acetic acid leaching tests	Korean standard leaching method	Korean standard leaching method	Korean standard leaching method
<b>pH</b>	6.0	5.6	11.0	5.8-6.3	6.0	-
<b>Pb(mg/l)</b>	0.019	-	0.12	0.045	0.0078	3.0
<b>Cr(mg/l)</b>	0.013	1.8	0.18	0.078	0.0260	1.5
<b>Cu(mg/l)</b>	0.014	-	0.048	0.055	0.0020	1.0
<b>Fe(mg/l)</b>	0.6	-	0.18	-	-	-
<b>Ni(mg/l)</b>	0.067	-	0.08	-	0.0046	-
<b>Zn(mg/l)</b>	0.02	-	0.61	0.105	0.0920	3.0
<b>Comparison of compressive strength</b>						
<b>compressive strength</b>	<b>This study</b>		<b>(Torres et al., 2017)</b>	<b>(Aggarwal &amp; Siddique, 2014)</b>	<b>(Kurama &amp; Kaya, 2008)</b>	<b>(Siddique, Singh, Belarbi, Ait-Mokhtar, &amp; Kunal, 2015)</b>
<b>Materials</b>	GGBFS+ FS (24.8%)	OPC	PCC+FS	Bottom fly ash +30%FS	Coal bottom ash5%+OPC	OPC+FS20%
<b>7<sup>th</sup> (MPa)</b>	19.0	16.5	39.2	19.36	28.02	30.9
<b>28<sup>th</sup>(MPa)</b>	22.2	18.5	48.4	31.81	40.38	45.3

\*FS foundry sand

## 5. Conclusion

This research work proposed that fine aggregate is to be partially replaced with waste foundry sand to preserve the natural resources in the process of making GPC structures. GPC comprises of 50% to 75% of fine and coarse aggregate, LCFA, GGBFS and alkaline solution. With ever increasing demand of fine aggregate, the replacement for fine aggregate (sand) in the construction field has become necessary due to the need to preserve natural resource of sand.

The optimized condition for the GPC maximum compressive strength was achieved through the analysis of the response surface plots designs and estimates the regression equation. On the 7<sup>th</sup> and 28<sup>th</sup> day, the predicted strengths under the D-optimal design were 18.8Mpa and 22.2Mpa, respectively, under the point prediction mixture percentage of 51.9 wt% fine aggregate, 24.8wt% foundry sand and 23.3wt% fly ash. Confirmatory runs for this result showed compression strength of 19.0Mpa and 22.2Mpa for the 7<sup>th</sup> and 28<sup>th</sup> days, respectively. Furthermore, the conventional concrete compressive strength is 16.5Mpa (7<sup>th</sup> day) and 18.5Mpa (28<sup>th</sup> day). This therefore verifies that the compressive strength of GPC is greater than that of the conventional concrete.

The use of fly ash, foundry sand and GGBFS contains heavy metals such as Zn, Fe, Cr, Ni, Pb and Cu. The analysis of the crystal structure and components of the ash incinerator showed that it was necessary to carry out the research for stabilizing and utilizing the ash incinerator in order to produce an eco-friendly construction material.

The total heavy metal concentration present in the fly ash is estimated by the MBA method. The highest concentration of Zn 11687.5mg/kg, Fe 14575mg/kg, Cu 35mg/kg, Ni 220mg/kg, and Cr 2412.5mg/kg, and Pb 46mg/kg was noted respectively. The contents of heavy metals in the ash were high. In this study, samples (R1-R14) were prepared by leaching test analysis using the KSLP method, and all test ratios showed leaching values (0.019mg/l Pb, 0.013mg/l Cr, 0.014mg/l Cu, 0.6mg/l Fe, 0.067mg/l Ni and 0.02mg/l Zn) being environmentally safe due to satisfying the Korean standard leaching requirements. It also indicates that GGBFS; waste foundry sand and fly ash combination can potentially reduce heavy metal leaching.

As a result of this study, it is confirmed that the characteristics according to the mixing ratio of fine aggregate, waste foundry sand, fly ash can be used efficiently as an eco-friendly construction material by increasing the value added aspect through recycling and reuse of by-product resources. However, prior to its use, incineration fly ash containing a lot of harmful substances may be subjected to potential leaching. Therefore, additional research is needed to be made in order to make it more stable and be utilized commercially. The current research of only a partial replacement of fine aggregate with foundry sand is done. D-optimal design was also used to make the GPC mixture design. Therefore, future works on a complete replacement of fine aggregate and improve the immobilization efficiency is recommended.



## REFERENCES

1. Abdel-Gawwad, H. A., & Abo-El-Enein, S. A. (2016). A novel method to produce dry geopolymer cement powder. *HBRC Journal*, 12(1), 13–24.
2. Aggarwal, Y., & Siddique, R. (2014). Microstructure and properties of concrete using bottom ash and waste foundry sand as partial replacement of fine aggregates. *Construction and Building Materials*, 54, 210–223. <https://doi.org/10.1016/j.conbuildmat.2013.12.051>
3. Associate, S. S. J., & Budhgaon, P. (2017). Beneficial Reuse of Waste Foundry Sand in Concrete, 7(3), 74–95.
4. Baek, J. W., Choi, A. E. S., & Park, H. S. (2017). Solidification/stabilization of ASR fly ash using Thiomer material: Optimization of compressive strength and heavy metals leaching. *Waste Management*. <https://doi.org/10.1016/j.wasman.2017.09.010>
5. Baker, D. E., & Amacher, M. C. (1982). Nickel, copper, zinc, and cadmium. *Methods of Soil Analysis. Part 2. Chemical and Microbiological Properties*, (methodsofsoilan2), 323–336.
6. Bakharev, T. (2006). Thermal behaviour of geopolymers prepared using class F fly ash and elevated temperature curing. *Cement and Concrete Research*, 36(6), 1134–1147. <https://doi.org/10.1016/j.cemconres.2006.03.022>
7. Bhardwaj, B., & Kumar, P. (2017). Waste foundry sand in concrete: A review. *Construction and Building Materials*, 156, 661–674. <https://doi.org/https://doi.org/10.1016/j.conbuildmat.2017.09.010>

8. Bilici Baskan, M., & Pala, A. (2010). A statistical experiment design approach for arsenic removal by coagulation process using aluminum sulfate. *Desalination*, 254(1–3), 42–48. <https://doi.org/10.1016/j.desal.2009.12.016>
9. Calle, M., Alho, P., & Benito, G. (2017). Channel dynamics and geomorphic resilience in an ephemeral Mediterranean river affected by gravel mining. *Geomorphology*, 285, 333–346. <https://doi.org/10.1016/j.geomorph.2017.02.026>
10. Choi, A. E. S., Roces, S., Dugos, N., Arcega, A., & Wan, M. W. (2017). Adsorptive removal of dibenzothiophene sulfone from fuel oil using clay material adsorbents. *Journal of Cleaner Production*, 161, 267–276. <https://doi.org/10.1016/j.jclepro.2017.05.072>
11. Choi, A. E. S., Roces, S., Dugos, N., Futralan, C. M., Lin, S. S., & Wan, M. W. (2014). Optimization of ultrasound-assisted oxidative desulfurization of model sulfur compounds using commercial ferrate (VI). *Journal of the Taiwan Institute of Chemical Engineers*, 45(6), 2935–2942. <https://doi.org/10.1016/j.jtice.2014.08.003>
12. Cohen, B., Cilliers, J. J., & Petrie, J. G. (1997). Optimization of solidification/stabilization treatment of ferro-alloy waste products through factorial design. *Journal of Hazardous Materials*, 54(3), 175–188.
13. Davidovits, J. (1994). Properties of geopolymer cements. In *First international conference on alkaline cements and concretes* (Vol. 1, pp. 131–149).
14. Dolage, D. A. ., Dias, M. G. ., & Ariyawansa, C. . (2013). Offshore Sand as a Fine Aggregate for Concrete Production. *British Journal of Applied Science & Technology*, 3(4), 813–825.

15. Eriksson, L., Johansson, E., & Wikström, C. (1998). Mixture design - Design generation, PLS analysis, and model usage. *Chemometrics and Intelligent Laboratory Systems*, 43(1–2), 1–24. [https://doi.org/10.1016/S0169-7439\(98\)00126-9](https://doi.org/10.1016/S0169-7439(98)00126-9)
16. Guo, B., Liu, B., Yang, J., & Zhang, S. (2017). The mechanisms of heavy metal immobilization by cementitious material treatments and thermal treatments: A review. *Journal of Environmental Management*.
17. Guo, B., Pan, D., Liu, B., Volinsky, A. A., Fincan, M., Du, J., & Zhang, S. (2017). Immobilization mechanism of Pb in fly ash-based geopolymer. *Construction and Building Materials*, 134, 123–130. <https://doi.org/10.1016/j.conbuildmat.2016.12.139>
18. Gurumoorthy, N., & Arunachalam, K. (2016). Micro and mechanical behaviour of Treated Used Foundry Sand concrete. *Construction and Building Materials*, 123, 184–190. <https://doi.org/10.1016/j.conbuildmat.2016.06.143>
19. Jiang, L., & Malhotra, V. (2000). Reduction in water demand of non-air-entrained concrete incorporating large volumes of fly ash. *Cement and Concrete Research*, 30(11), 1785–1789. [https://doi.org/10.1016/S0008-8846\(00\)00397-5](https://doi.org/10.1016/S0008-8846(00)00397-5)
20. Journal, I., Engineering, O. F., For, A., & Sustainable, E. (2015). Foundry sand; utilization as a partial replacement of fine aggregate, 4(1), 308–311.

21. Khan, M. S. H., Castel, A., Akbarnezhad, A., Foster, S. J., & Smith, M. (2016). Utilisation of steel furnace slag coarse aggregate in a low calcium fly ash geopolymer concrete. *Cement and Concrete Research*, 89, 220–229. <https://doi.org/10.1016/j.cemconres.2016.09.001>
22. Kurama, H., & Kaya, M. (2008). Usage of coal combustion bottom ash in concrete mixture. *Construction and Building Materials*, 22(9), 1922–1928. <https://doi.org/10.1016/j.conbuildmat.2007.07.008>
23. Li, X., Ouyang, J., Xu, Y., Chen, M., Song, X., Yong, Q., & Yu, S. (2009). Optimization of culture conditions for production of yeast biomass using bamboo wastewater by response surface methodology. *Bioresource Technology*, 100(14), 3613–3617. <https://doi.org/10.1016/j.biortech.2009.03.001>
24. Madhavan, S., & Vijayprakash, M. (2016). Experimental Investigation on Utilization of Flyash and Waste Foundry Sand as a Partial Replacing Material in Concrete, 6(4), 4222–4224. <https://doi.org/10.4010/2016.969>
25. Mangialardi, T., Paolini, A. E., Poletini, A., & Sirini, P. (1999). Optimization of the solidification/stabilization process of MSW fly ash in cementitious matrices. *Journal of Hazardous Materials*, 70(1), 53–70.
26. Moon, H.-Y., Choi, Y.-W., Song, Y.-K., & Jeon, J.-K. (2005). Fundamental properties of Mortar and Concrete using waste foundry sand. *Journal of the Korea Concrete Institute*, 17(1), 141–147.

27. Muteki, K., MacGregor, J. F., & Ueda, T. (2007). Mixture designs and models for the simultaneous selection of ingredients and their ratios. *Chemometrics and Intelligent Laboratory Systems*, 86(1), 17–25. <https://doi.org/10.1016/j.chemolab.2006.08.003>
28. NDTV. Tamil Nadu bureaucrat shunted for crackdown on illegal sand mining. Retrieved from [https://www.youtube.com/watch?v=gEy\\_FIDCyDQ](https://www.youtube.com/watch?v=gEy_FIDCyDQ)
29. Osada, M., Tanigaki, N., Takahashi, S., & Sakai, S. I. (2008). Brominated flame retardants and heavy metals in automobile shredder residue (ASR) and their behavior in the melting process. *Journal of Material Cycles and Waste Management*, 10(2), 93–101. <https://doi.org/10.1007/s10163-007-0204-y>
30. Pavani, A., Rakesh, J., Gopichand, P., & Professor, A. (2016). Conventional Concrete over GEO Polymer Concrete Using GGBS. *International Journal of Engineering Science and Computing*, 6(4), 3647–3651. <https://doi.org/10.4010/2016.845>
31. Rajshekhar, M. SAND MINING. Scroll.in. <https://doi.org/2017>
32. Rajshekhar, M. Sand Mining in Tamil Nadu. Retrieved from [https://www.youtube.com/watch?v=\\_7E2-I3ddgY](https://www.youtube.com/watch?v=_7E2-I3ddgY)
33. Rao, F., & Liu, Q. (2015). Geopolymerization and its potential application in mine tailings consolidation: A review. *Mineral Processing and Extractive Metallurgy Review*, 36(6), 399–409. <https://doi.org/10.1080/08827508.2015.1055625>

34. Roviello, G., Ricciotti, L., Ferone, C., Colangelo, F., Cioffi, R., & Tarallo, O. (2013). Synthesis and characterization of novel epoxy geopolymer hybrid composites. *Materials*, 6(9), 3943–3962. <https://doi.org/10.3390/ma6093943>
35. Saviour, M. N. (2012). Environmental impact of soil and sand mining: a review. *International Journal of Science, Environment and Technology*, 1(3), 125–134.
36. Saviour, M. N., & Stalin, P. (2012). Soil and Sand Mining: Causes, Consequences and Management. *IOSR Journal of Pharmacy (IOSRPHR)*, 2(4), 1–6.
37. Sengupta, D. (2014). *Recent Trends in Modelling of Environmental Contaminants*. Springer.
38. Siddique, R., & Noumowe, A. (2008). Utilization of spent foundry sand in controlled low-strength materials and concrete. *Resources, Conservation and Recycling*, 53(1–2), 27–35. <https://doi.org/10.1016/j.resconrec.2008.09.007>
39. Siddique, R., Schutter, G. de, & Noumowe, A. (2009). Effect of used-foundry sand on the mechanical properties of concrete. *Construction and Building Materials*, 23(2), 976–980. <https://doi.org/10.1016/j.conbuildmat.2008.05.005>
40. Siddique, R., & Singh, G. (2011). Utilization of waste foundry sand (WFS) in concrete manufacturing. *Resources, Conservation and Recycling*, 55(11), 885–892. <https://doi.org/10.1016/j.resconrec.2011.05.001>

41. Siddique, R., Singh, G., Belarbi, R., Ait-Mokhtar, K., & Kunal. (2015). Comparative investigation on the influence of spent foundry sand as partial replacement of fine aggregates on the properties of two grades of concrete. *Construction and Building Materials*, 83, 216–222. <https://doi.org/10.1016/j.conbuildmat.2015.03.011>
42. Son, J. H., Baek, J. W., Choi, A. E. S., & Park, H. S. (2017). Thiomer solidification of an ASR bottom ash: Optimization based on compressive strength and the characterization of heavy metal leaching. *Journal of Cleaner Production*, 166, 12–20. <https://doi.org/10.1016/j.jclepro.2017.07.113>
43. Subramonia Pillai, N., Kannan, P. S., Vettivel, S. C., & Suresh, S. (2017). Optimization of transesterification of biodiesel using green catalyst derived from AlbiziaLebbeck Pods by mixture design. *Renewable Energy*, 104, 185–196. <https://doi.org/10.1016/j.renene.2016.12.035>
44. Swanson, H. E., & Tatge, E. (1951). Standard x-ray diffraction patterns. *Journal of Research of the National Bureau of Standards*, 46(4), 318. <https://doi.org/10.6028/jres.046.036>
45. Torres-Carrasco, M., & Puertas, F. (2015). Waste glass in the geopolymer preparation. Mechanical and microstructural characterisation. *Journal of Cleaner Production*, 90, 397–408. <https://doi.org/10.1016/j.jclepro.2014.11.074>

46. Torres, A., Bartlett, L., & Pilgrim, C. (2017). Effect of foundry waste on the mechanical properties of Portland Cement Concrete. *Construction and Building Materials*, 135, 674–681. <https://doi.org/10.1016/j.conbuildmat.2017.01.028>
47. Vijai, K., Kumutha, R., & Vishnuram, B. G. (2010). Effect of types of curing on strength of geopolymer concrete. *International Journal of the Physical Sciences*, 5(9), 1419–1423. Retrieved from <http://www.academicjournals.org/IJPS>
48. Zhuang, X. Y., Chen, L., Komarneni, S., Zhou, C. H., Tong, D. S., Yang, H. M., Wang, H. (2016). Fly ash-based geopolymer: Clean production, properties and applications. *Journal of Cleaner Production*, 125, 253–267. <https://doi.org/10.1016/j.jclepro.2016.03.019>